

# Shuttle Retrun-To-Flight IH-108 Aerothermal Test at CUBRC – Flow Field Calibration and CFD

Kei Y. Lau<sup>1</sup>

*Boeing Company, St. Louis, Missouri, 63166*

*and*

M.S. Holden<sup>2</sup>

*CUBRC, Buffalo, New York, 14225*

**This paper discusses one specific aspect of the Shuttle Retrun-To-Flight IH-108 Aerothermal Test at CUBRC, the test flow field calibration. It showed the versatility of the CUBRC LENS II wind tunnel for an aerothermal test with unique and demanding requirements. CFD analyses were used effectively to extend the test range at the low end of the Mach range. It demonstrated how ground test facility and CFD synergy can be utilized iteratively to enhance the confidence in the fidelity of both tools. It addressed the lingering concerns of the aerothermal community on use of impulse facility and CFD analysis. At the conclusion of the test program, members from the NASA Marshall (MSFC), CUBRC and USA (United Space Alliance) Consultants (The Grey Beards) were asked to independently verify the flight scaling data generated by Boeing for flight certification of the re-designed external tank (ET) components. The blind test comparison showed very good results.**

## Nomenclature

$a = \sqrt{\gamma R_g T}$	Speed of Sound
$c_p$	Specific Heat of Air at Constant Pressure, Btu/lb <sub>m</sub> -°R
$c_v$	Specific Heat of Air at Constant Volume, Btu/lb <sub>m</sub> -°R
$C_h$	Stanton Number
$C_{h_{ref}}$	Stagnation Point Stanton number
$C_{h_{\infty}}$	Free Stream Stanton number
$C_{p_i}, C_p$	Static Pressure Coefficient for the Local Condition
$h_i/h_u$	Shock Interference Heating Factor
$H_{aw}$	Adiabatic Wall Enthalpy, Btu/lb <sub>m</sub>
$H_t$	Total Enthalpy, Btu/lb <sub>m</sub>
$H_w$	Wall Enthalpy, Btu/lb <sub>m</sub>
$L$	Length, inches or feet
$M, Ma, Mach$	Mach Number
$M_e$	Boundary Edge Mach Number
$M_L$	Boundary Edge Mach Number
$p_e$	Pressure at the Boundary Layer Edge, psia or psfa
$p_t, p_{t1}$	Total or Settling Pressure, psia or psfa
$p_{t2}$	Pitot Pressure in Test Section, psia or psfa
$p_{t3}$	ET Nose Spike Pressure, psia or psfa
$p_{\infty}, p$	Free Stream Static Pressure, psia or psfa
$Pr_w$	Prandtl Number at the Wall

<sup>1</sup> Technical Fellow, Boeing Military Airplane, P. O. Box 516, Mail Code , St. Louis, MO, Senior Member.

<sup>2</sup> Program Manager, AAEC, CUBRC, 4455 Genesee Street, Buffalo, NY, Fellow.

$q_{\infty}$	Free Stream Dynamic Pressure, psi or psf
$r$	Recovery Factor
$R$	Radius, ft
$R_g$	Gas Constant per Unit Mass
$Re$	Reynolds Number
$Re_{\theta}$	Momentum Thickness Reynolds Number
$St$	Stanton Number
$St_{ref}, St (ref)$	Stagnation Point Stanton Number
$St_{\infty}$	Free Stream Stanton Number
$T_{aw}$	Adiabatic Wall Temperature, °R
$T_o, T_O, T_0$	Total Temperature, °R
$T_t$	Total Temperature, °R
$T_w, T_w$	Model Wall Temperature, °R
$T_{\infty}, T$	Free Stream Static Temperature, °R
$v_{\infty}, v$	Free Stream Velocity, ft/sec
$x/L$	Longitudinal Position as a Fraction of the Reference Length
$\alpha$ , Alpha	Angle of Attack, degrees
$\beta$ , Beta	Angle of Sideslip, degrees
$\gamma$	Ratio of Specific Heats, $c_p/c_v$
$\mu_{\infty}, \mu$	Free Stream Dynamic Viscosity, slugs/ft-sec
$\mu_e$	Dynamic Viscosity at the Boundary Layer Edge, slugs/ft-sec
$\mu_w$	Dynamic Viscosity at the Wall, slugs/ft-sec
$\nu$	Kinematic Viscosity, slugs/ft-sec
$\theta$	Boundary Layer Momentum Thickness
$\rho_{\infty}, \rho$	Free Stream Density, slugs/ft <sup>3</sup>
$\rho_e$	Density at the Boundary Layer Edge, slugs/ft <sup>3</sup>

### ***Subscripts***

aw	Adiabatic Wall Condition
e	Boundary Layer Edge Condition
i	Subscript Denoting Local Conditions
inf	Free-Stream Condition
L	Boundary Layer Edge Condition
o	Total Condition
ref	Stagnation or Reference Condition
t	Total Condition
w	Wall Condition
$\infty$	Free Stream Condition

## **I. Introduction**

The STS-107 Columbia accident has necessitated the need to re-evaluate the Space Shuttle Vehicle (SSV) design. The Columbia Accident Investigation Board concluded that foam shed during ascent from external tank impacted leading edge of the left wing causing damage. One of the re-design is to remove Bipod fitting TPS foam ramp to eliminate debris source. The bare metal bi-pod fitting was never flown before without TPS cover. It is one of the most critical components in the Shuttle Return-to-flight re-design effort. Boeing is under subcontract to United Aerospace Alliance (USA) to provide the aerothermal environment for the bi-pod fitting and associated components.

In July 2004, NASA management approved the request to conduct the IH-108 aerothermal wind tunnel test and made it a Return-to-flight requirement. With a March 2005 launch schedule, it meant that the test team had less than five months to develop and conduct the test and test data analysis. The details of the bi-pod re-design challenge and its aerothermal environment generation was reported in the full test report submitted to NASA by Boeing<sup>1</sup>. The test program at CUBRC was reported in an earlier AIAA paper<sup>2</sup>. This presentation will focus on the preparations for the IH-108 test and a summary discussion of the test data evaluation.

## II. The IH-108 Test Program

The IH-108 aerothermal wind tunnel test is conducted at the CUBRC LENS-II shock tunnel at fully duplicated Mach 3.5 and Mach 4 flight conditions using a 3.5% scale integrated vehicle model. The total model length measured 84.5 inches long. The CUBRC tunnel allowed testing at actual flight Mach number, Reynolds number and enthalpy or enthalpy ratio for the first time in Shuttle program history. The heat flux gage is unique because it can be customized to test components as small as 0.040" in size for the 3.5% scale model. The test data set provided detailed heating environment data of small components that never had direct data before. It discovered several "hot spots" around the bi-pod structure that could not be resolved before. The test data had been used to verify the bi-pod aerothermal environment and updated the analysis model. It is used to help certified that the new bi-pod design is safe to fly the STS-114 mission.

### A. CUBRC test facility simulates actual flight parameters

In order to develop design heating models (or Body Points (BPs)), the test conditions needed to simulate Performance Enhancement Certification (PE-Cert) Trajectory level parameters such as Reynolds number, Mach number, pressure, etc. for the range of peak heating in the ET bipod fitting region. Data were also needed at actual flight conditions to develop an improved, more accurate flight-scaling factor for the new heating models. The STS-4 and STS-7 Best Estimated Trajectories (BETs) were used along with the design trajectory to define the ranges for each parameter that were to be tested to successfully complete the previously defined objectives.

### B. Special gage and instrumentation of small components

In order to achieve the aforementioned test objectives, it was required for the selected test facility to be able to obtain pressure data as well as heat transfer data, especially in the ET bipod fitting region. In addition, the test facility should be able to install instruments on small protuberances such as the ET bipod fitting, struts and yoke, as well as the LO<sub>2</sub> feed line acreeage and bracket near the ET bipod. In order to reduce the uncertainty in the heating environments for the ET bipod region, a high-fidelity full-stack (Orbiter, External Tank, Solid Rocket Boosters) wind tunnel model was required to simulate the complex flow field in this area. Thus, the External Tank (ET) model needed to simulate all major protuberances upstream and in the vicinity of the ET bipod, including the Intertank stringers (corrugated surface), LO<sub>2</sub> and LH<sub>2</sub> Protuberance Air Load (PAL) ramps, LO<sub>2</sub> cable tray and Ice/Frost ramps, and LH<sub>2</sub> feed line. These protuberances as well as the complex ellipsoidal shape of the ogive were to simulate the latest ET configuration (ET-123). Figure 1 provides an overview of the External Tank.

In addition to the level of detail, the model scale was also required to be greater than that used for previous tests (0.0175-scale). This was necessary to allow sufficient instrumentation be installed on the small protuberances and surrounding acreeage in order to better understand the flow characteristics and heating gradients that resulted from the ET bipod redesign. The selected test facility was required to provide the appropriate test conditions and at the same time accommodate the 0.035-scale wind tunnel model. CUBRC LENS II had the unique capability to test at the desired test conditions (Mach range, Re/ft and  $T_w/T_o$ ) and the data acquisition capability (both pressure and heating data) based on proven methods.

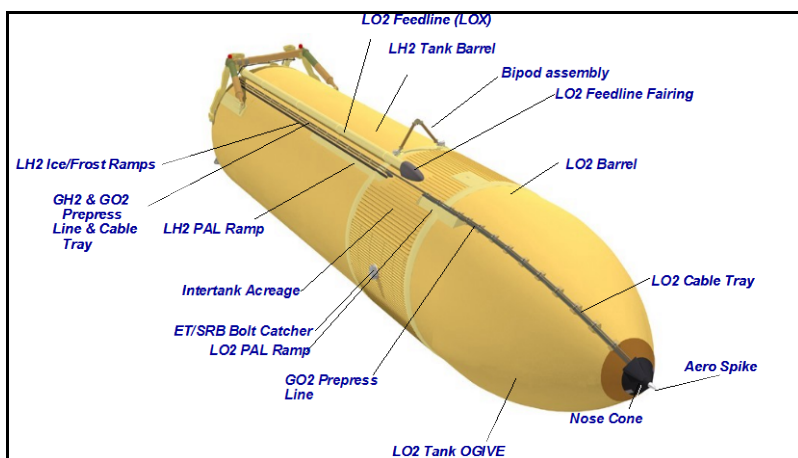


Figure 1, Overview of External Tank Configuration

### C. Data reduction and quality in LENS II Tunnel

During the past 15 years, two large new ground test facilities, LENS I and II, have been constructed by CUBRC and successfully employed to directly replicate flight conditions on full-scale interceptors flying at velocities from 3,000 ft/sec to 15,000 ft/sec at altitudes from 10,000 to 200,000 ft. The construction of these wind tunnels was driven by the need to conduct fundamental research as well as design and evaluate hypersonic vehicles whose performance were controlled by complex flow phenomena, such as boundary layer transition, compressible turbulent shear layer mixing, shock/turbulence interaction and “real gas” combustion chemistry, all of which are poorly understood and cannot be accurately predicted. Furthermore, such flows cannot be easily scaled. For example, the non-equilibrium fluid dynamic and chemical process which occurs in regions of boundary layer transition and “real gas” flow chemistry can only be replicated with any accuracy on full-scale test articles under fully duplicated free-stream conditions. The LENS II tunnel was constructed specifically to conduct full-scale testing of high speed vehicle systems that operate at velocities from 3,000 ft/sec to 7,000 ft/sec at altitudes from 10,000 ft. to 120,000 ft. The tunnel has been used in aeroheating studies conducted with full-scale vehicles at full-duplicated flight conditions for the Standard Missile, HyFly, and X-51 programs and provided aerothermal heating and dynamic shroud separation data that directly duplicates those heating environments that are generated under actual flight conditions.

### III. Flow-field calibration and blockage test

The test conditions to be simulated in the proposed IH-108 test program were discussed in full IH-108 test report<sup>1</sup>. Based on the free-stream conditions for the selected Performance Enhancements Certification (PE Cert) trajectory, the peak convective heating for the full-stack, integrated-vehicle OTS configuration on and around the bipod fitting occurs when the Mach number is close to 4.0. The LENS II facility provided the only tunnel capable of replicating the required Mach numbers, Reynolds numbers, and Total Enthalpy. To match the Reynolds number based on the vehicle length and the free-stream conditions for the PE Cert trajectory, the unit Reynolds number in the CUBRC LENS II facility should be  $7.727 \times 10^6$  per foot. To match the Reynolds number based on the vehicle length and the free-stream conditions for the STS-4 trajectory, the unit Reynolds number in the CUBRC LENS II facility should be  $2.65 \times 10^6$  per foot. A third test condition was proposed to simulate the Reynolds number for the Mach 4 tests (IH-97) that were conducted in the 1980s in AEDC’s Aero Thermal Tunnel C<sup>3</sup>. To match the Reynolds number based on the length of the 0.0175-scale AEDC model and the free-stream conditions for these tests, the unit Reynolds number in the CUBRC LENS II facility should be two million per foot.

Since all of the previous tests in the CUBRC LENS II facility were conducted at velocities higher than the Mach 4.0 required by the IH-108 test program, two new throats were designed and fabricated by CUBRC specifically for the IH-108 tests. One nozzle was to deliver Mach 4 flow in the test section; the second was to deliver Mach 3.5 flow. The design of these new throats was optimized using full Navier-Stokes solutions with chemical reactions. Before the IH-108 test program, a series of airflow calibration tests were conducted. These calibration runs were conducted:

- 1) to establish the flow properties over the range of test conditions,
- 2) to calibrate the numerical tools available to fluid dynamics analysts by comparing the measurements from a series of calibration runs with the computed flow field solutions, and
- 3) to ensure that the boundary layer was fully turbulent in the wind-tunnel simulations just as the boundary layer was fully turbulent in flight. In addition it was important to match the ratio of boundary layer thickness to bipod height.
- 4) to look for evidence of flow blockage caused by the presence of a large model

A model simulating the forward section of the External Tank (ogive) was built, instrumented, and used in these calibration runs to check for turbulent flow. See Figure 2 and Figure 3. In addition, two blockage test runs were also conducted before the IH-108 test program. For these blockage tests, the full-stack (OTS) configured model was used, with a small number of gauges hooked up in the forward section of the elements (Orbiter, ET, SRBs). The IH-108 test required CUBRC to design tunnel hardware employing DPLR nozzle solutions to attain the desired conditions. The nominal exit Mach number for the LENS-II Mach 3.5 – 7.0 nozzle is 4.5, so the throat diameter of the nozzle was increased to bring the test Mach number down to a value of 4.0 for the first part of the test, and then again to 3.5 for the second part. The design of the throat modifications for the Mach 3.5 and 4.0 conditions were guided by computations with the DPLR code to produce satisfactory flow profile close to the target condition. During each calibration run, a rake of Pitot probes was placed in the free-stream just beyond the nozzle exit plane in the same x-location as the IH-108 bipod assembly to assess flow uniformity. High-frequency pressure instrumentation is used in the pitot probes. However, in regions where flows generate high thermal loads, thermal

protection systems were employed which lowered the frequency response. Total temperature measurements were made in the lower enthalpy flows with shielded thermocouple probes while total heat transfer measurements were made with miniature thin-film or coaxial instrumentation placed in the stagnation region of a hemispherical nosetip.

Pitot pressure is used as one measure of free-stream accuracy because: (1) it is a directly measurable quantity, and (2) it is sensitive to the momentum and velocity fluctuations in the flow field. Hence, it is an important, primary indicator by which to judge flow quality against desired standards of accuracy. From the Pitot tube and hemisphere stagnation temperature measurements, it is possible to determine the accuracy of the free-stream dynamic pressure and the stagnation point enthalpy to  $\pm 5\%$  and the Mach number to  $\pm 1.5\%$ .

These results are now compared with the precalibration computational results. Figure 4 shows an example of the comparison of the Navier-Stokes and the measured pitot profile measurements for Mach 4.0, demonstrating the level of agreement obtained between CFD and experiment in the IH-108 test program.



**Figure 2, LENS II IH-108 Flow Field Survey Rake**



**Figure 3. LENS II Calibration Ogive Model As Installed In Calibration Rake**

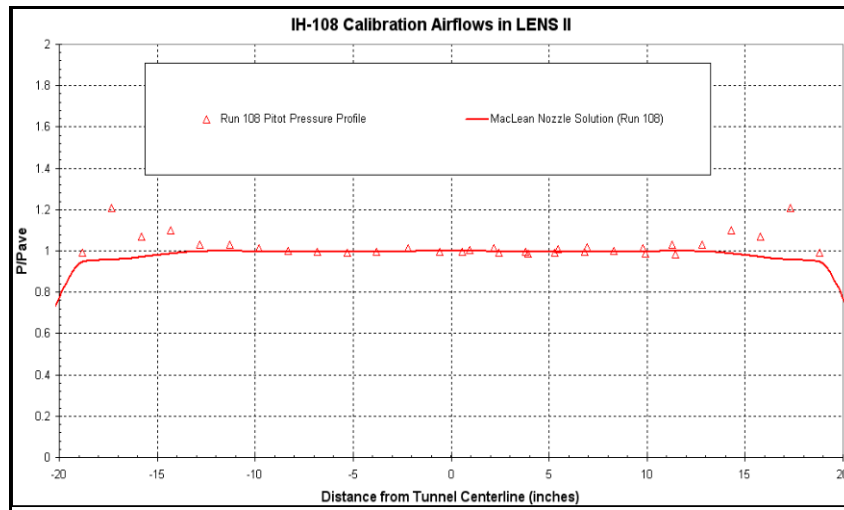


Figure 4, Mach 4.0 Nozzle CFD Solution – Pitot Pressure Profile for IH-108 Test Conditions

#### IV. Numerical Tools for Generating Computational Fluid Dynamics Flow Fields

The availability of pressure and heat transfer data on a calibration ET ogive model prior to the actual IH-108 complete model test provided a tremendous opportunity for pre-test run condition evaluation. The Boeing team completed six (6) model scale ET ogive CFD runs before the calibration test. The Boeing pre-test runs used the projected free-stream conditions from CUBRC and were slightly different from the actual calibration conditions. NASA-JSC and CUBRC both generated CFD solutions from the “as run” calibration conditions. All ET CFD runs discussed in this section were run with a truncated, clean ET ogive (no protuberance components). The computational tools used by each team, as well as the studies/modifications performed to optimize their output, are discussed in this section.

##### A. Boeing – WIND

The CFD tool used by the Boeing team is the BCFD code, which has both structured and unstructured grid options. For this study, the structured grid WIND code was used. The WIND code was originally developed by Boeing as a general purpose CFD tool and is currently supported by NPARC Alliance<sup>4</sup>. The code supports multiple-zone handling with patched, overlapped or point-matched boundaries. It is a node-based finite volume algorithm with Van Leer, Roe, HLLC schemes and TVD options. The code is 2<sup>nd</sup> order spatial accurate and can be implicit or explicit in each direction. Local time stepping, time-accurate and global Newton iteration options are available. It can be run using ideal gas, Liu-Vinokur equilibrium air model, frozen flow or finite rate chemistry. Available turbulence models include Baldwin-Lomax<sup>5</sup>, Spalart-Allmaras one-equation<sup>6</sup>, Menter SST<sup>7</sup>, and Chien k- $\epsilon$ <sup>8</sup>. For the current study, axi-symmetric 2-D and 3-D solutions were run, using Roe 2<sup>nd</sup> order scheme with TVD using a factor of 1. All turbulent runs were done with the SST model.

The computational grid for the three shuttle bodies is shown in Figure 4. The ET forward section is a tri-cone fitted to an ogive where strong shock-shock interaction was expected to cause massive flow separation around the tri-cone nose tip, or aero spike. The ET ogive grid was divided into four zones, which allowed the solutions to capture the diverse shock structure and still converge rapidly. The near surface zones used a high-density grid with slow stretching to assure good heat transfer results. This strategy proved to be very successful. Most solutions of the ET ogive were obtained overnight on single CPU Windows workstations without waiting for Linux cluster availability.

In order to get good heat transfer results at the Mach/altitude combination of the PE Cert trajectory test conditions, the initial grid had a 0.0001-inch cell spacing off the surface based on previous Boeing experience. This spacing was found to be too tight and caused the solution not to converge sufficiently. The heat transfer magnitude and trend were all within expectation, but the distribution curve showed a “stair step” shape. A grid optimization study was conducted to find an optimal value of the  $Y^+$  that would provide a smoother distribution of heat transfer and boundary layer properties in the stream-wise direction and, at the same time, a fast convergence of the solution. The original grid had a target cell Reynolds number ( $Y^+$ ) of 0.1 and was found to cause convergence problems. Several  $Y^+$  values were tested from 0.1 to 1.0. All  $Y^+$  values larger than 0.5 were found to be too loose, resulting in



an 18% over prediction in heat transfer. The  $Y^+$  values of 0.2-0.3 were found to be optimal for this study. It must be emphasized that this grid study is not universal, but it is tailored to the specific ET ogive and the associated test conditions.

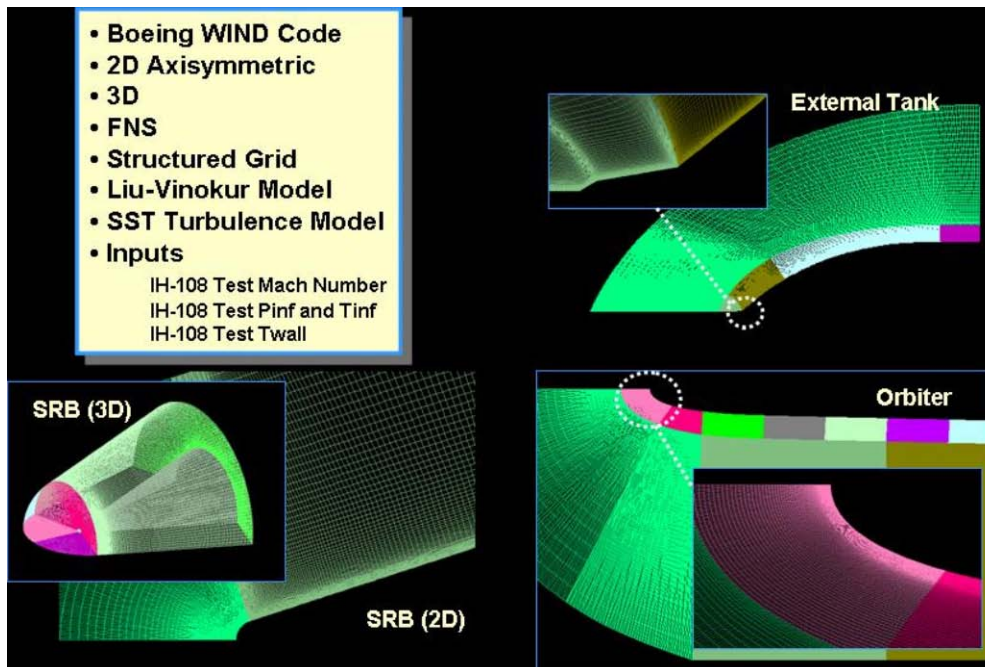


Figure 5. Boeing CFD Multiple Zone Grid Topology

A quick examination of the Mach contour revealed that the solution using the revised grid captured the shock structure and the compression corner separation with good fidelity, as shown in Figure 5. Figure 6 and Figure 7 compare the magnitude of the separation showing the distinctive shock structure between laminar and turbulent flow around the aero spike.

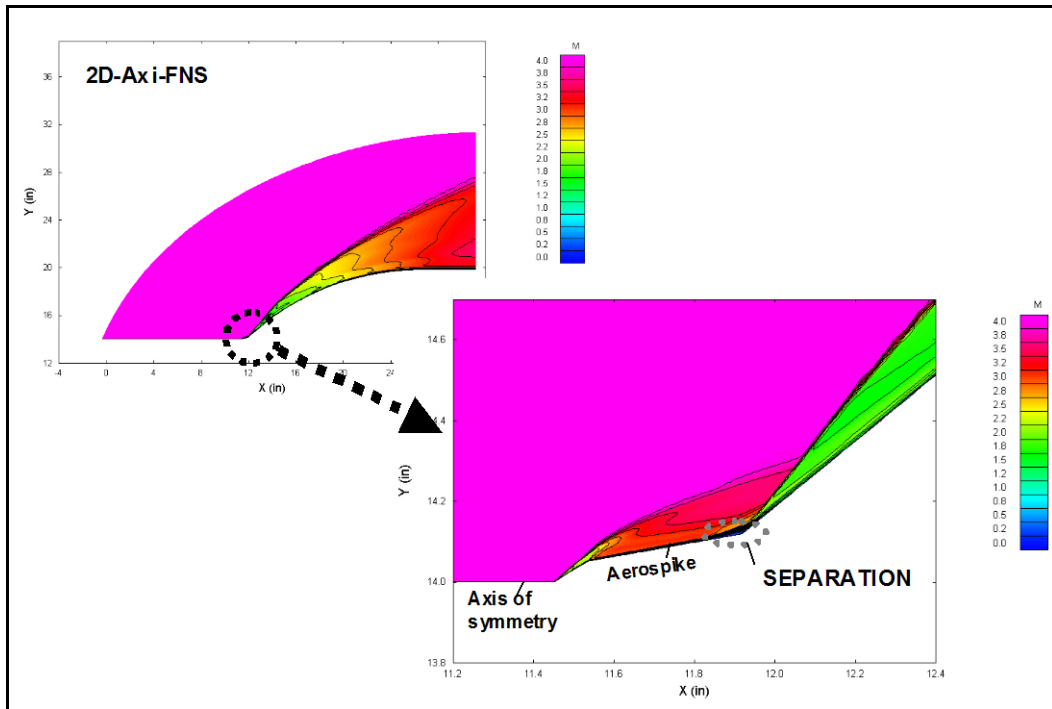


Figure 6. Typical ET Ogive Mach Number Contour in Mach 4.0 Turbulent Flow

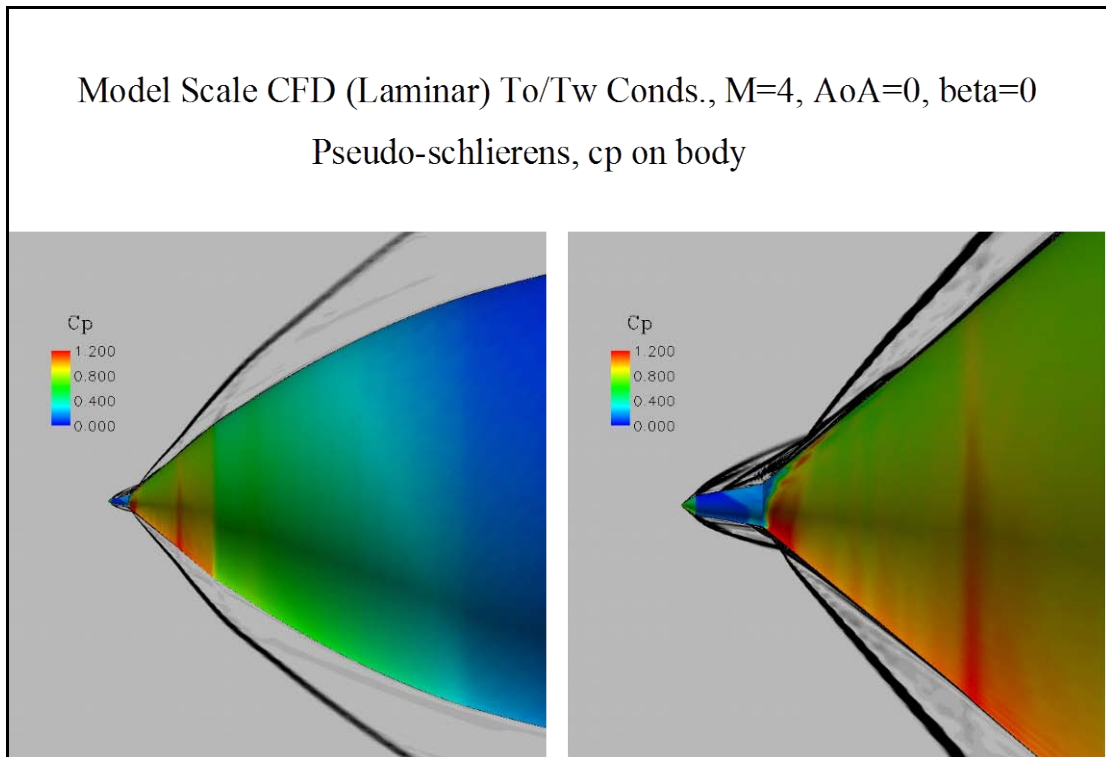
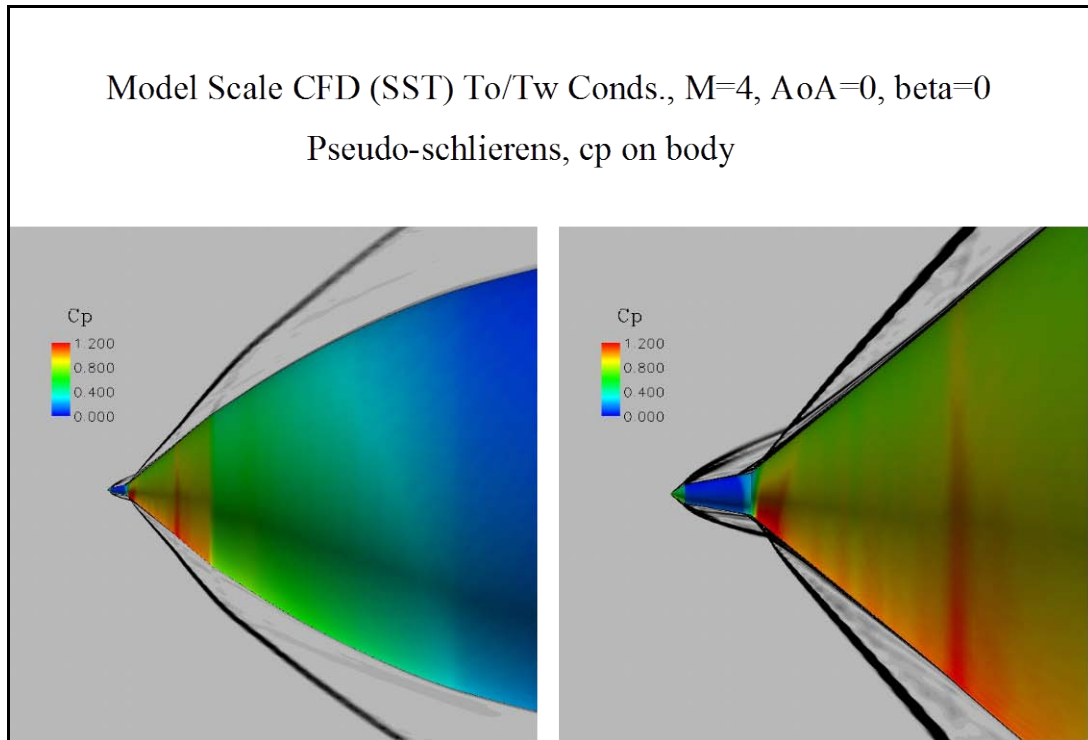


Figure 7. Laminar CFD Solution at Aerospike Junction





**Figure 8. Turbulent CFD Solution at Aerospike Junction**

### B. NASA JSC – OVERFLOW

The NASA CFD analysis performed on the IH-108 calibration runs was done using the OVERFLOW code<sup>9,10</sup> on the ET ogive axi-symmetric grid. Each case was run fully turbulent using Menter's SST two-equation turbulence model<sup>7</sup>. The grid was truncated at  $X_T = 562.5$  inches, just in front of the interaction region, to obtain undisturbed heating rates. Using the axi-symmetric assumption minimized the grid size to 360,000 points, which allowed a single condition to be run on one CPU in approximately 16 to 20 hours.

### C. CUBRC - DPLR

The primary tool used by the CUBRC team is the Data Parallel Line Relaxation (DPLR) code<sup>11</sup> provided by NASA Ames Research Center. This code is a multi-block, structured solver that solves the full Navier-Stokes equations for two-dimensional, axi-symmetric, or three-dimensional flows. The code capabilities include vibrational, electronic, and rotational non-equilibrium, fully coupled, finite rate chemistry, as well as coupled radiation. Many of these thermo-chemical capabilities were not employed in this particular program. DPLR is a finite volume code with a modified (low dissipation) Steger-Warming flux splitting approach for the convection terms<sup>12</sup> and second-order central differencing for the diffusion terms. Turbulence models include the Baldwin-Lomax algebraic model<sup>5</sup> and the Menter-SST 2-equation model<sup>7</sup>, both of which are corrected for compressibility<sup>13</sup>. Data parallel line relaxation is used for time integration, providing an exceptionally fast and stable convergence behavior.

Several issues related to uncertainties and errors in the numerical computations were investigated. Iterative convergence was also considered. The surface heat transfer is shown for several different iteration steps with DPLR in Figure 8. The algorithm used by DPLR is known to be very stable and converge much better than most other codes. Figure 8 shows that iterative convergence error is negligible for these calculations.

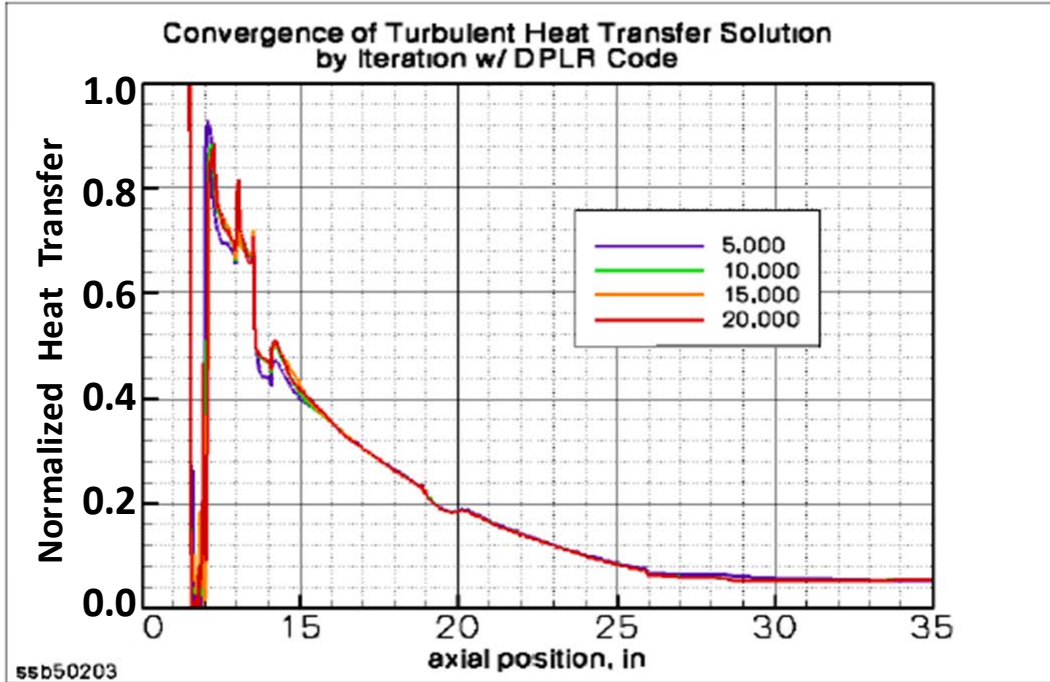


**Figure 9, Effect of Iteration Steps on DPLR CFD Heat Transfer Results**

Grid convergence error, or ordered discretization error, is typically the most significant uncertainty in a CFD calculation. Assessment of this error is usually addressed by sequencing the grid one or more times, meaning that every other point is removed from the grid in all directions, doubling the size of all grid cells. The converged solution for three sequence levels of the grid is shown in Figure 9. These results show some grid dependency in the tri-cone region where the flow separates and reattaches, but on the cylindrical part of the geometry, the solution is consistent across all three grids. Figure 10 shows the turbulent  $y^+$  spacing at the wall for each of those same three grids. This dimensionless quantity is an important parameter in turbulence modeling for CFD. The result of this analysis shows that the DPLR code is quite insensitive to grid sizing  $y^+$  values and that a level as much as 4.0 can be tolerated without any drastic loss of accuracy in the prediction of flow entering the interaction region. It also demonstrates that as few as 293 by 75 points is sufficient to provide an accurate answer up to the interaction region of the External Tank. For this study, turbulent  $y^+$  lies within range of independence with DPLR and is nominally 1, as shown in Figure 11.

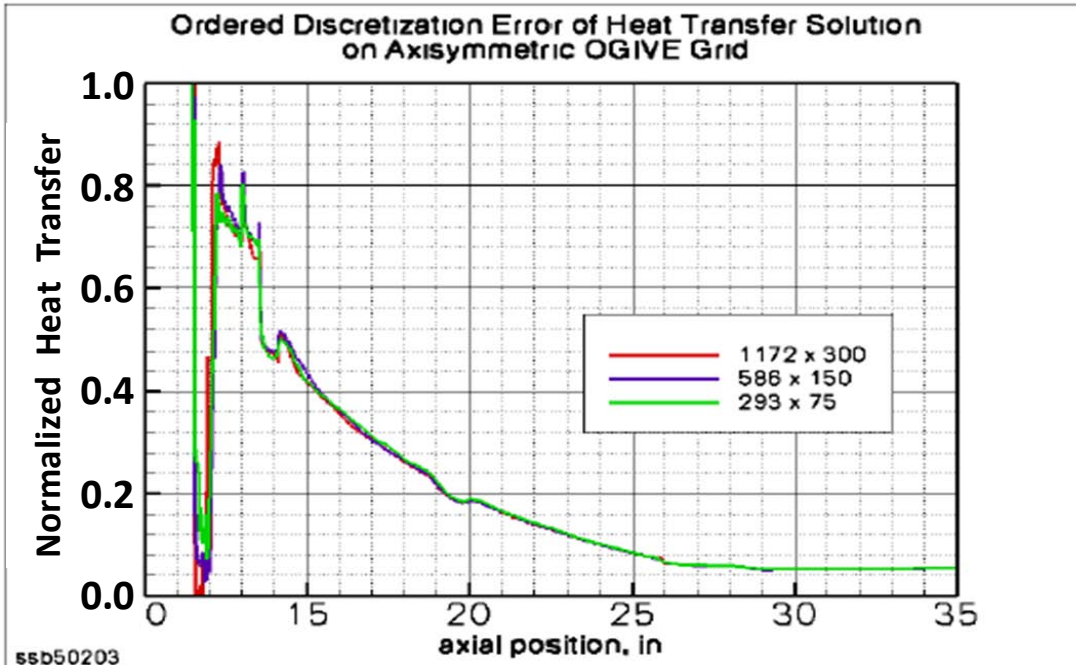


Figure 10, Negligible Discretization Error of DPLR CFD Heat Transfer Results

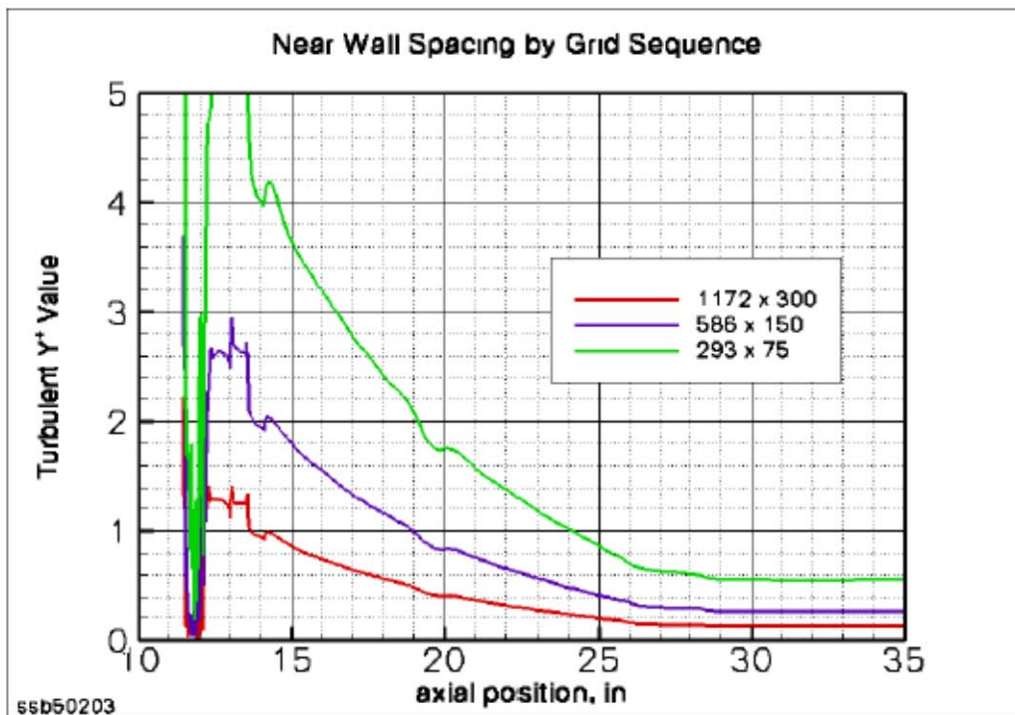


Figure 11, Y+ Spacing for 3 Grid Densities of DPLR CFD Results

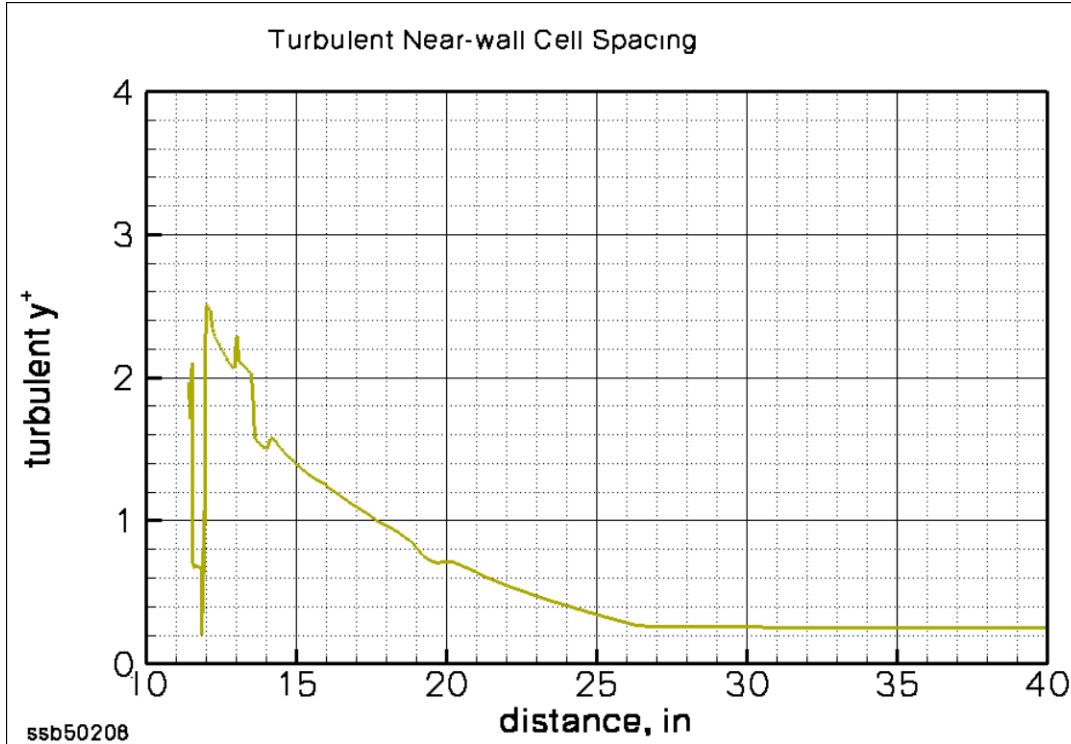


Figure 12, Turbulent Y+ Selected for DPLR Tool

## V. External Tank Ogive Pre-Test Data Comparison with CFD Predictions

A calibration ogive was installed during the facility checkout phase of the program to determine the boundary layer state on the ET model. The calibration ogive was designed to capture the basic geometry of the actual ogive without the detailed 3-D features. This calibration model was designed as a perfectly axi-symmetric body that follows a typical profile of the nose cone of the shuttle external fuel tank. Pre-test calibration runs were only available for the Mach 4.0 conditions, as the Mach 3.5 calibration runs were done after the Mach 3.5 phase of the test. This was done since the Mach 4.0 calibration runs had been extremely successful, and the expectation was that the same results would be obtained at this other Mach number setting. This decision was also taken to ensure Mach 3.5 data would be available on time to develop the required heating environments for vehicle certification. The heat-transfer measurements from the Mach 4 calibration runs are compared with the computed Stanton numbers defined by free stream conditions.

$$St = \frac{qdot}{\rho_{\infty} V_{\infty} c_p (T_{aw} - T_w)}$$

Calibration flow-field runs were conducted for all test conditions used in the IH-108 test program with the calibration ogive and at alpha/beta angles of 0°. For the first phase (Phase 1), most of the runs were performed at Mach 4.0 and Reynolds number representing the PE Cert No-Fail trajectory condition based on the 3.5% model scale. For this Reynolds number, Mach 4 data were obtained at conditions that simulated the flight total enthalpy (Test Condition (TC) #2), or the wall-to-total temperature ratio (TC #1). Runs at a Reynolds number/ft of 2 million at Mach 4.0 were also included to compare with previous 0.0175-scale model test results (TC #3). A Reynolds number/ft of 2.65 million for Mach 4.0 was also tested for comparison with STS-4 DFI data (TC #6). Calibration runs at an intermediate wall-temperature ratio (TC #5) and an intermediate Reynolds number (TC #4) were also obtained as backups.

### A. Boeing – WIND

The first six runs were conducted using CUBRC provided pre-test conditions. They included flight scale calculations to help assess boundary layer scaling parameter selection. These conditions were slightly different from the “as run” conditions; therefore, the comparisons were made using dimensionless parameters such as pressure coefficient ( $C_p$ ) and Stanton number ( $St$  or  $C_h$ ).

The pressure results from the Mach 4.0 calibration runs are shown in Figure 13 in the form of pressure coefficient ( $C_p$ ). The magnitude and trend of the pressure data looked good, but there was more data scatter than we usually expect from pressure measurements at this facility ( $\Delta C_p$ 's of 0.07 to 0.16 from run to run).

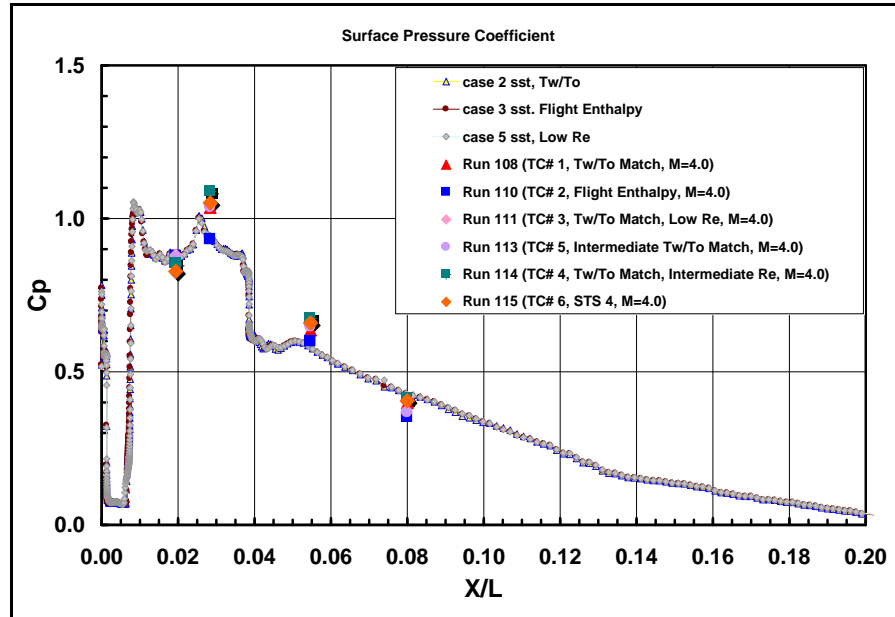


Figure 13, WIND Code Pre-Test CFD Pressure Comparison with Calibration Runs

The heat transfer results were also compared for each run to assess the boundary layer state at individual test conditions. Calibration Run 108, TC #1, at PE Cert Reynolds number and wall temperature ratio is represents the primary condition used to obtain aeroheating data for the bi-pod fitting environment update. The comparison clearly showed that the boundary layer on the ET ogive is turbulent at this condition. Calibration Run 110, TC #2, at PE Cert Reynolds number and flight total enthalpy also showed fully turbulent boundary layer. However, the heat transfer comparison of TC #2 in Stanton number did not match as well as TC #1. For the low Reynolds number cases (Run 111 and blockage test, TC #3), the Stanton number comparison showed excellent agreement in heat transfer and a solid turbulent boundary layer.

Figure 14 shows the overall pre-test comparison of three CFD runs and seven test runs using Stanton number times the  $1/5^{\text{th}}$  power of the local Reynolds number,  $Re_x$ . The three CFD solutions seemed to collapse on each other very well despite the wide range of Reynolds number and total pressure. The agreement between test data and CFD is very good, with a general over-prediction by the CFD results, as shown in Figure 14. Based on these results, it was determined that the desired test conditions had been simulated, and sufficient calibration data were available to validate this conclusion.

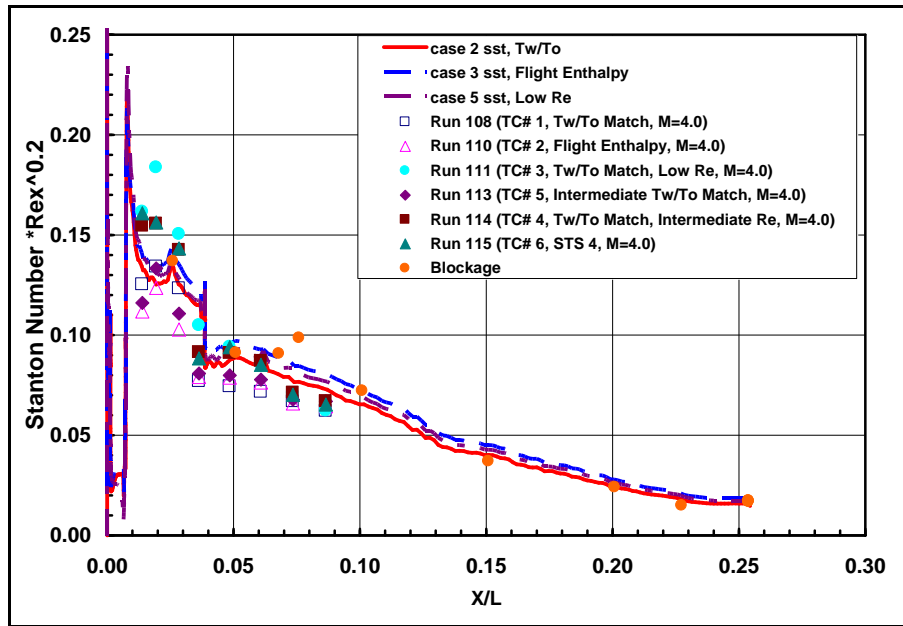


Figure 14, WIND Code Heat Transfer Pre-Test CFD Comparison for All Runs

### B. NASA JSC – OVERFLOW

The first cases analyzed were the Mach 4 calibration runs. Initially, the targeted free-stream conditions were used to try and get some pre-test predictions for the heating. After the calibration runs were made, the actual free-stream conditions were used to re-run the cases.

There is good agreement between the wind tunnel measurements and the CFD results for the calibration ogive in the Mach 4 air stream. This agreement indicates that the free-stream conditions in the wind tunnel had been adequately calibrated.

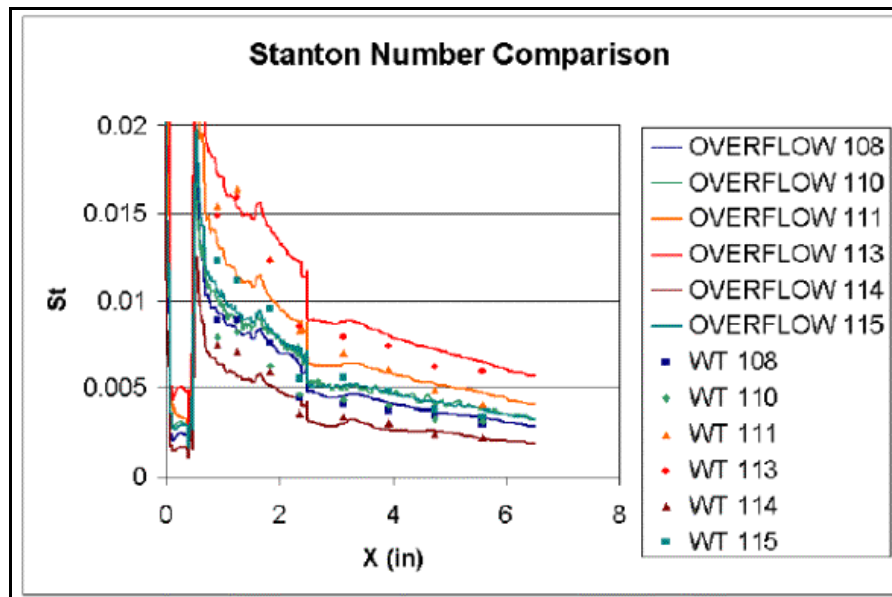


Figure 15, NASA-JSC Overflow Stanton Number Comparison for Mach 4.0 Calibration Runs

### C. CUBRC - DPLR

The calculation for the calibration ogive was made using DPLR and the solution was compared to several runs in the facility. The flow-field for this geometry is shown in Figure 16, which gives the computational schlieren of the



model on the top half of the figure and the experimental schlieren on the bottom half. The comparison shows agreement within the resolution of the camera. A detailed close-up of the computational schlieren is shown in Figure 17 in the complex tri-cone region of the flow-field. This level of detail was not attainable during the experiments with the available resolution of the camera. However, it is important to understand these shock interaction patterns, as the reattached flow-field downstream is defined by the pattern in this region.

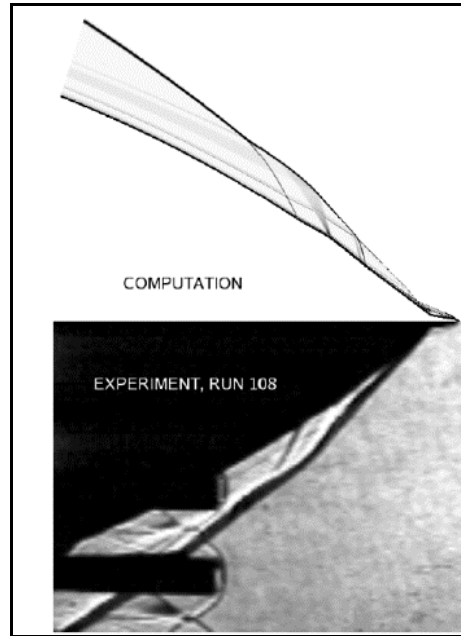


Figure 16, DPLR Computational Schlieren Compared to Experimental Result

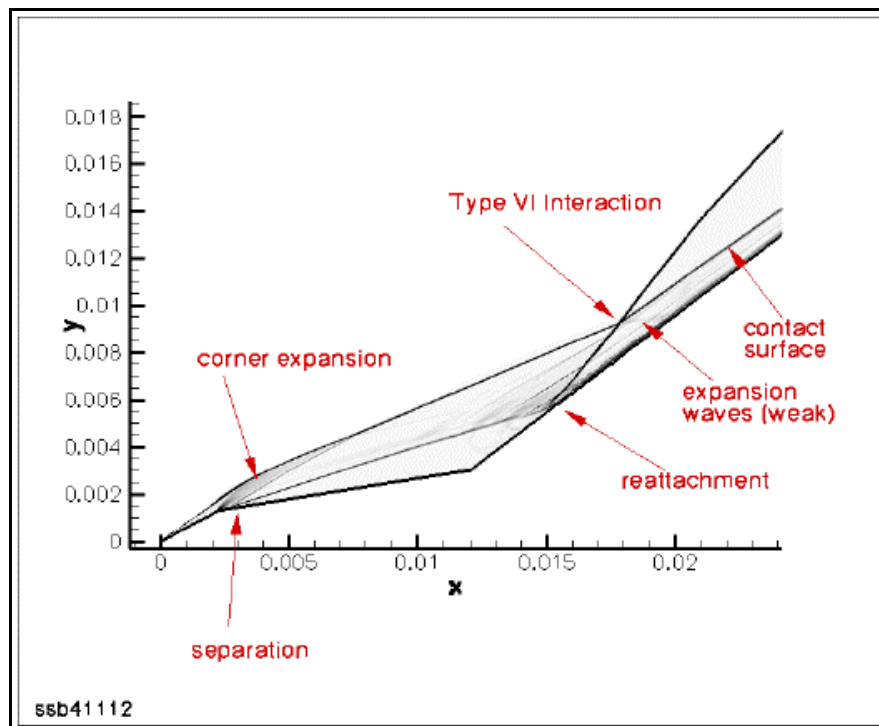


Figure 17, DPLR Detailed Close-Up of the Computational Schlieren

The heat transfer solutions for the calibration runs are shown in Figure 18 in non-dimensional form. The most significant conclusion is that the heat transfer data trends for all run conditions are consistent with the fully turbulent computational solution and the laminar solution lies far below the data. This confirms that the flow transitions to turbulent immediately downstream of the separation reattachment.

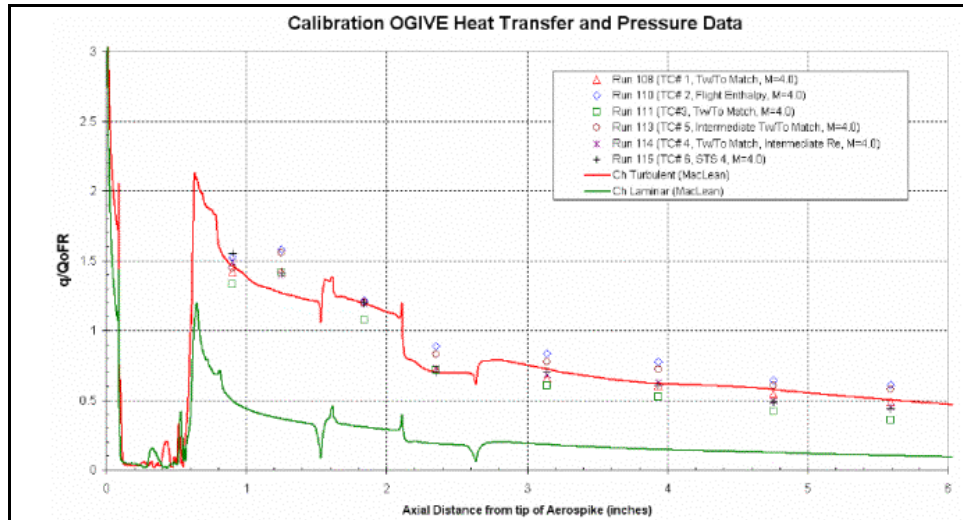


Figure 18, CUBRC DPLR CFD Comparison for All Mach 4.0 Conditions

## VI. Flow Interference and Blockage

From the outset, the planners of the IH-108 test program focused on a model that was as large as possible to enable the instrumentation of small protuberances such as the bipod fitting. Since the scale of the integrated-vehicle model that had served as the workhorse of previous aeroheating wind-tunnel test programs was 0.0175, the planners focused on having the model scale for the IH-108 program be in the range of 0.030 to 0.035. Due to the size of the model, there was concern among some members of the test team, especially the senior advisory group, that the test data could be affected by blockage.

To alleviate these concerns, the test facility (CUBRC) performed a pre-test study to demonstrate that no blockage or other interference effects would be seen. The placement of a 0.035-scale model of the full-stack IH-108 model in the nozzle flow field for the Mach 4.0 tests is shown in Figure 19, which shows computational schlieren of the nozzle (i. e., wind tunnel) flow field with the model super-imposed on it. The boundary layer along the nozzle walls is visible, as are the expansion waves from the acceleration of the flow into the test section. It is clear that the forward portions of the External Tank and of the Orbiter, as well as the bipod region, are free of any interactions that might disrupt the core flow.

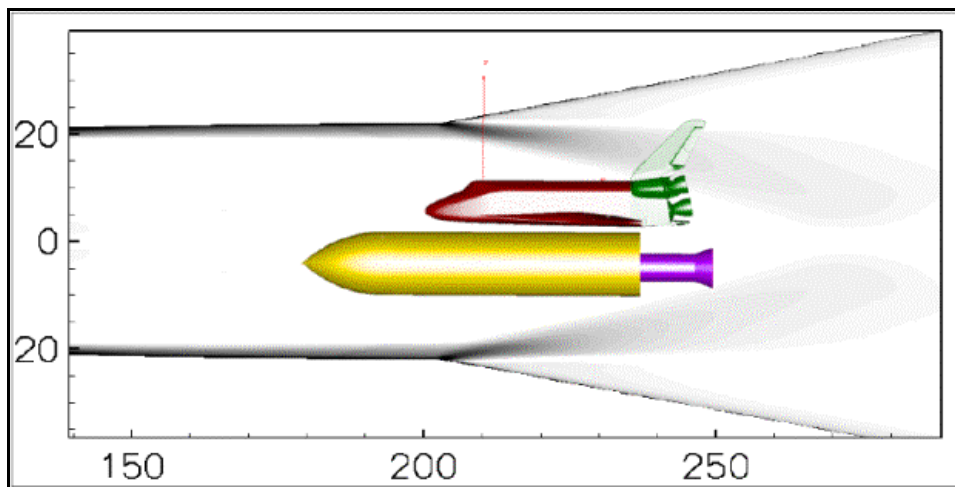


Figure 19, Mach 4.0 Nozzle CFD Schlieren Plot with Super-Imposed Test Model

In addition to the pre-test flow interference analysis performed by CUBRC, two blockage test runs were conducted at Mach 4 at the low Reynolds number of  $2.0 \times 10^6/\text{ft}$  to explore the capability to detect blockage effects experimentally. The blockage effect, if any, would be detected by abnormal surface gauge measurement. The actual test model, with some modifications, was used as the blockage model. These tests were conducted at Mach 4 because the nozzle throat was already in place from the calibration tests. The blockage tests also served to detect boundary layer transition on the three model elements (ET, Orbiter and SRBs).

The blockage test model was a partially instrumented IH-108 test model. Eight (8) heat-transfer gauges and three (3) pressure transducers on the ET ogive from the original instrumentation list were connected. Five (5) heat-transfer gauges and seven (7) surface pressure transducers were added to the ogive before the blockage test started. Five (5) pairs of heat-transfer gauges and pressure transducers were used to determine the location of an undisturbed flow area that could be used as a reference heat transfer location. A total of thirteen (13) heat-transfer gauges and ten (10) surface pressure transducers were activated on the ET ogive.

Six (6) heat-transfer gauges were installed on the lower centerline of the Orbiter, while five (5) heat-transfer gauges were added to the  $270^\circ$  ray of the solid rocket booster (SRB). These gauges were added to determine the boundary layer state on the forward location of these components. All gauges used in the blockage test remained active in all subsequent phases of the test program.

The pressure distribution measured on the External Tank of the blockage model in the Mach 4 air-stream is compared in Figure 20 with the pressure distributions computed using a variety of flow models. Note that the computed pressure distribution is essentially independent of the assumed flow model. That is, the computed surface-pressure distribution is the same whether the boundary layer is assumed to be laminar or fully turbulent and both for the appropriate total temperature and for the appropriate wall-to-total-temperature ratio. The upstream-most pressure gage on the blockage model is located at approximately the same  $x/L$  coordinate as the downstream-most pressure gage on the calibration-ogive model (see Figure 20). The resulting pressure coefficients for these two runs at this “common  $x/L$  station” are in relatively good agreement. The agreement is reiterated in Figure 21, where the Blockage run heat transfer data is plotted against the calibration data for the low  $Re/\text{ft}$  case (Run 111).

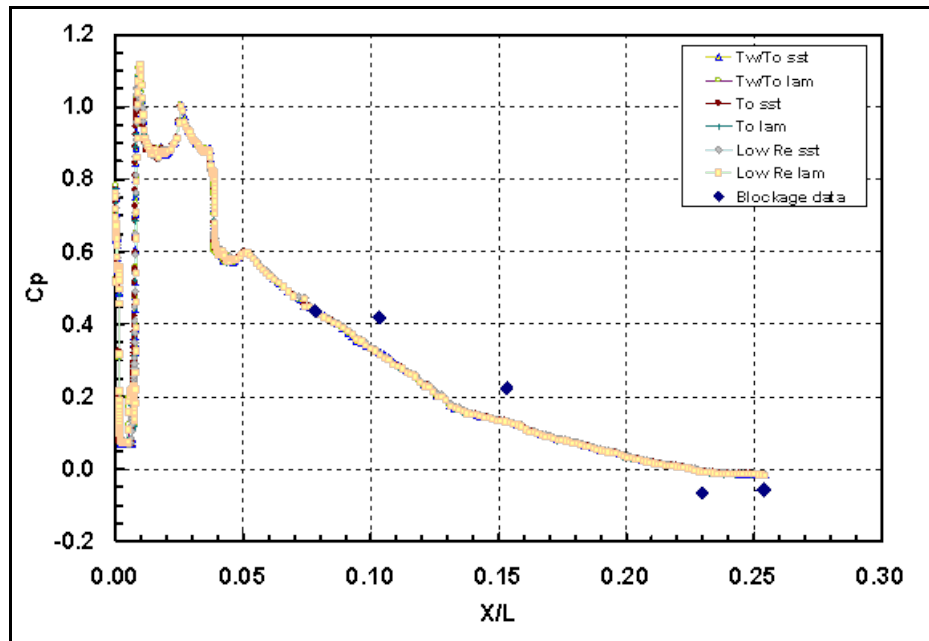


Figure 20, Boeing WIND Code Pre-Test CFD Solution Pressure Comparison with Blockage Run

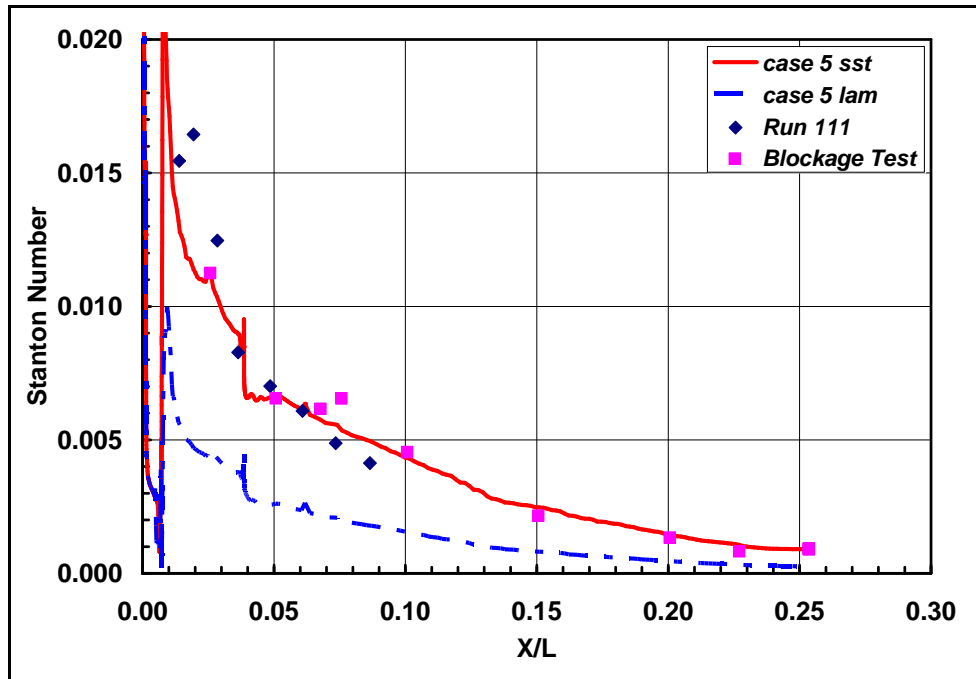


Figure 21, WIND Code Pre-Test CFD Comparison at Low Re/ft (2 million) Condition

## VII. Boundary Layer State Analysis

For the IH-108 Test Program, one of the principal questions to be answered through the analysis of the calibration data was to ensure that the boundary layer characteristics in the wind-tunnel simulations accurately represented those seen in flight.

In earlier ground tests of OTS configuration, such as the 0.0175-scale model of the integrated vehicle for the IH-97 test<sup>3</sup>, the boundary layers on the External Tank, on the Orbiter and on the SRBs were tripped to assure turbulent flow to obtain conservative aeroheating data. Questions were raised early in the IH-108 test program about the need to implement tripping. The NASA consultants (The Greybeards team) unanimously opposed using any boundary layer trips in the IH-108 test, as the planned test conditions would simulate actual flight parameters and, in turn, the resulting flow conditions would be representative of those seen in flight. However, there were different opinions about how soon the flow would transition to turbulent. The Boeing team conducted a quick study prior to the test, using both an engineering aeroheating code and CFD before the test program to assess this problem. Simple and individual axi-symmetrical models of the ET, Orbiter and SRBs were used in the analyses to obtain answers regarding the boundary layer transition in a timely manner. During the test period, the CUBRC team conducted a more comprehensive CFD study using 3-D models. The results of these studies and their comparison to the test data are discussed in this section.

The value of  $Re_\theta/M_e$  (Momentum thickness Reynolds number divided by the local, edge Mach number) was used to assess boundary layer transition behavior. In flight, the transition onset value for a sharp cone is 150 and for the Shuttle Orbiter is 280. In the CUBRC test facility, more conservative values of 125 and 220, respectively, are usually used. The ET nose section is an ogive shape similar to the Orbiter windward surface, so it was expected that the Orbiter onset criterion would apply to the ET. The SRB, in turn, is a slightly blunted cone-cylinder. Thus, the cone transition criterion should apply to the SRB.

The Boeing pre-test CFD cases included both laminar and turbulent runs at similar free-stream conditions. The Orbiter windward surface and SRB nosecone were also run in the same free-stream conditions. These flow fields were computed to assess the boundary layer state of all component bodies and to determine the need for boundary layer trips.

The heat transfer measurements on the ET ogive confirmed that the flow was fully turbulent immediately downstream from the location where the nose tip bow shock impinged on the ogive surface. From the calibration test schlieren pictures in Figure 16, it can be determined that the separation at the tri-cone compression corner was limited, which clearly indicated a turbulent flow field behavior early on.

From the above analyses and the calibration test data, the members of the IH-108 test team were confident that turbulent boundary layer existed on the ET surface for all test conditions. Thus, it was established that boundary layer trips were not required for the External Tank model.

### VIII. Conclusion

1. The requested free-stream test conditions were achieved within a reasonable range. The Mach 4.0 throat produces a very uniform test section Mach core with variation of 1% for 5 of the test conditions and one condition at 2% (Run 110, TC #2).
2. For the Mach 4.0 test conditions, the agreement between calibration test data and CFD is very good. The test team felt confident that the desired test conditions had been simulated and sufficient calibration data were available to corroborate it.
3. The calibration run heat transfer measurements on the ET ogive confirmed that the flow was fully turbulent immediately downstream from the location where the nose tip bow shock impinged on the ogive surface. Turbulent boundary layer also exists on the Orbiter windward surface in all test conditions. No boundary layer trip should be required for the ET or Orbiter model. The boundary layer state on the SRB, on the other hand, was not clearly defined by the test data.
4. The availability of ET ogive pressure and heat transfer data before the actual test commenced provided a tremendous opportunity for pre-test run condition evaluation.
5. All new test conditions using either new or existing nozzle hardware should be calibrated before the actual test is performed.
6. Good agreement among the CFD solutions from Boeing, NASA/JSC and CUBRC team was shown. The predictions are consistent at all Mach 4 conditions and typically over-predicted the test data by 10% to 20% on the ET ogive.

### Acknowledgments

Kei Y. Lau will like to dedicate this paper to the late Professor John J. Bertin who took a personal interest in the synergy of ground test facility and CFD analysis. He personally marked up the Chapter 6 of the IH-108 Final Report which is the basis of this paper. The successful completion of the IH-108 wind tunnel test was due to the dedicated teamwork and hard work that was performed by the IH-108 team that consisted of personnel from Boeing, USA, NASA, CUBRC, Everfab, the Greybeard Committee, Lockheed-Martin and USA/SRB. I am particularly grateful to the Greybeard Committee team members who included Del Freeman (lead), Paul Romere, Dick Neumann, John Bertin, Bass Redd, and Vince Zoby, who provided valuable advice and guidance that were critically important to the success of this test.

### References

- <sup>1</sup>Lopez, Pedro, Lau, Kei Y. and Wong, Dexter J., "IH-108 Post-Test Analysis Report for the Space Shuttle Aeroheating Wind Tunnel Test at the CUBRC LENS II Facility", Boeing Report No. NS05HOU341, November 18, 2005.
- <sup>2</sup>T.P. Wadhams, M.G. MacLean, M.S. Holden, and G.J. Smolinski, "Return to Flight Testing of a 3.5% Scale Space Shuttle OTS and OT Model at Mach Numbers of 3.5 and 4.0", AIAA Paper 2006-720, 44<sup>th</sup> AIAA Aerospace Sciences Meeting and Exhibit, January 9-12, 2006, Reno, Nevada.
- <sup>3</sup>Nutt, K. W., Matthews, R. K., and Best, J. T., Jr., "Analysis of Heat-Transfer Measurements on the Shuttle External Tank Obtained in Two AEDC Wind Tunnels", AIAA-86-0774-CP, AIAA 14<sup>th</sup> Aerodynamic Testing Conference, West Palm Beach, FL, Mar. 1986.
- <sup>4</sup>NPARC Alliance, WIND CFD Code, version 5, website, <<http://www.grc.nasa.gov/WWW/winddocs/wind5.0/index.html>>.
- <sup>5</sup>Baldwin, B.S. and Lomax, H., "Thin Layer Approximation and Algebraic Model for Separated Turbulent Flows". AIAA Paper 78-0257. Huntsville, AL: 1978.
- <sup>6</sup>Spalart, P.R. and Allmaras, S.R., "A One-Equation Turbulence Model for Aerodynamic Flows". AIAA Paper 92-0439. 30<sup>th</sup> Aerospace Sciences Meeting & Exhibit. Reno, NV: 6-9, Jan. 1992.
- <sup>7</sup>Menter, F.R., "Two-Equation Eddy-Viscosity Turbulence Models for Engineering Applications". AIAA Journal. Vol. 32, no 8. Pgs 1598 – 1605. August 1994.

- <sup>8</sup> Chien, K.-Y., "Predictions of Channel and Boundary-Layer Flows with a Low Reynolds Number Turbulence Model," *AIAA Journal*, Vol. 20, No. 1, Jan. 1982, pp. 33-38.
- <sup>9</sup> Buning, P., Jespersen, D., Pulliam, T., Klopfer, G., Chan, W., Slotnick, J., Krist, S. and Renze, K. (2000), *OVERFLOW User's Manual, Version 1.8s*, NASA Langley Research Center, 2000.
- <sup>10</sup> Jespersen, D. C., Pulliam, T. H., and Buning, P. G. (1997), "Recent Enhancements to OVERFLOW," *AIAA 35th Aerospace Sciences Meeting*, Reno, NV: Paper 97-0644, January 1997.
- <sup>11</sup> Wright, M.J.; Bose, D., and Candler, G.V. (1998), "A Data Parallel Line Relaxation Method for the Navier-Stokes Equations". *AIAA Journal*. Vol. 36, No. 9, pp. 1603 – 1609. Sept. 1998.
- <sup>12</sup> MacCormack, R.W. and Candler, G.V. (1989), "The Solution of the Navier-Stokes Equations Using Gauss-Seidel Line Relaxation". *Computers and Fluids*. Vol. 17, No. 1, pp. 135 – 150, 1989.
- <sup>13</sup> Brown, James (2002), "Turbulence Model Validation for Hypersonic Flows". *AIAA Paper 2002-3308*. 8TH Thermophysics and Heat Transfer Conference. St. Paul, MN, pp. 24 – 26, June 2002.



# Shuttle Retrun-To-Flight IH-108 Aerothermal Test at CUBRC – Flow Field Calibration and CFD

Kei Y. Lau  
Boeing Technical Fellow  
(314) 233-2947  
[Kei.y.lau@boeing.com](mailto:Kei.y.lau@boeing.com)

Michael S. Holden  
Program Manager, AAEC, CUBRC  
(716) 204-5115  
[holden@cubrc.org](mailto:holden@cubrc.org)

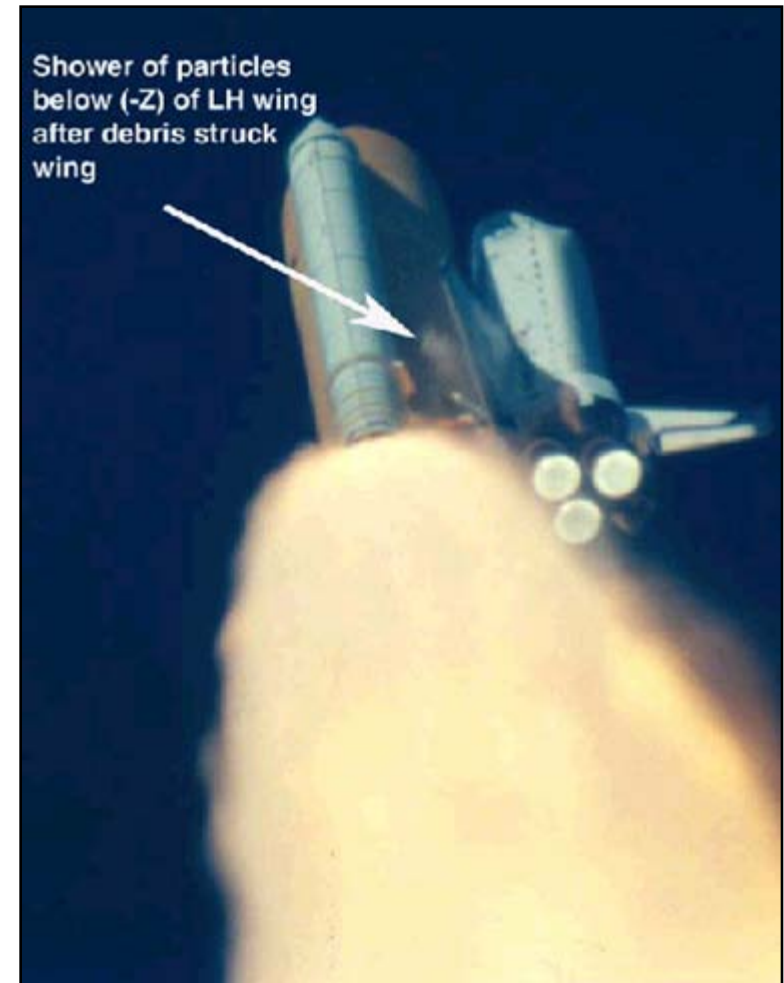
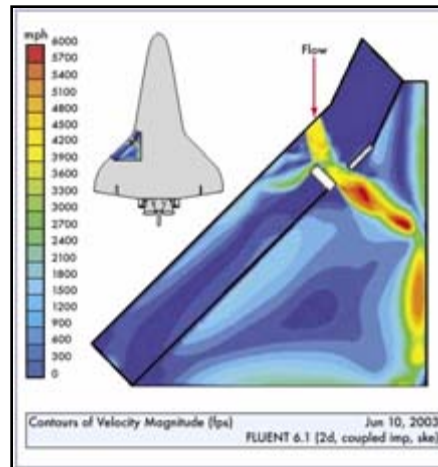
**AIAA Paper 2011-  
Session 151-FD-29: Hypersonic Facilities and Measurements**

**41st AIAA Fluid Dynamics Conference and Exhibit  
June 27-30, 2011 – Honolulu, Hawaii**

# The Columbia Accident

## The Physical Cause

- Foam shed during ascent from external tank impacted leading edge of the left wing causing damage
- Superheated gas entered wing structure during re-entry causing failure of the wing



# Design Changes - Bipod Fitting

- Bipod Fitting ramp removed to eliminate debris source

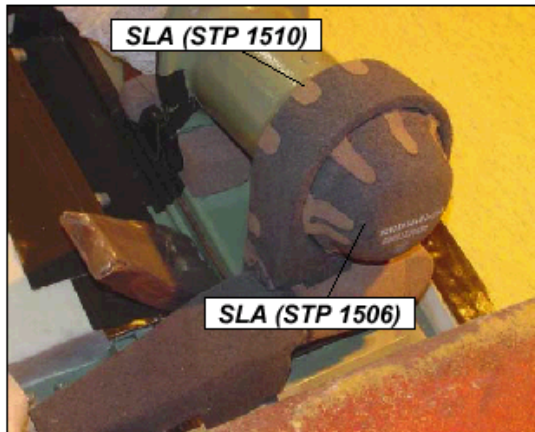
- Bare metal fitting has never been flown

- Bipod fitting most critical component under the redesign effort

- Complex flow field exist
- No direct test or flight data exist for this component for full stack vehicle



Redesigned Bipod



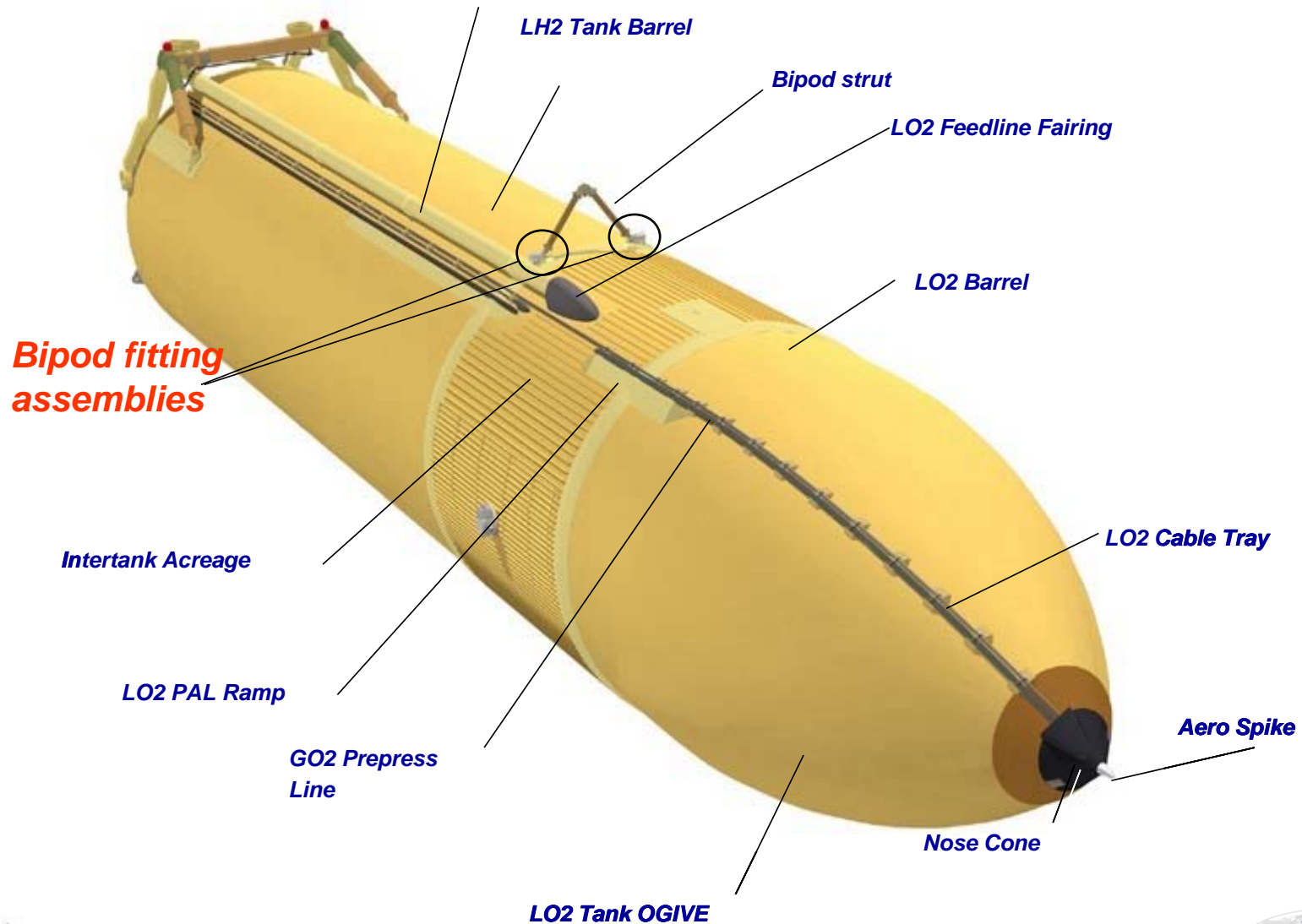
Bipod Housing  
(Prior to Foam Application)



Bipod Ramp  
(After Final Foam Trim)

Configuration used  
up to STS-107

# External Tank Overview



# Flow-field calibration and blockage test

- **This Part of the IH-108 Test Program Addressed the Lingering Concerns Of the Aerothermal Community On Use Of Inpulse Facility And CFD Analysis**
- **Establish The Flow Properties Over The Range Of Test Conditions**
- **Calibrate The Numerical Tools Available To Fluid Dynamics Analysts By Comparing The Measurements From A Series Of Calibration Runs With The Computed Flow Field Solutions**
- **Ensure That The Boundary Layer Was Fully Turbulent In The Wind-tunnel Simulations Just As The Boundary Layer Was Fully Turbulent In Flight. In Addition It Was Important To Match The Ratio Of Boundary Layer Thickness To Bipod Height**
- **Look For Evidence Of Flow Blockage Caused By The Presence Of A Large Model**



# Flow Field Survey Rake and Calibration Ogive Model

Advanced Global Strike Systems

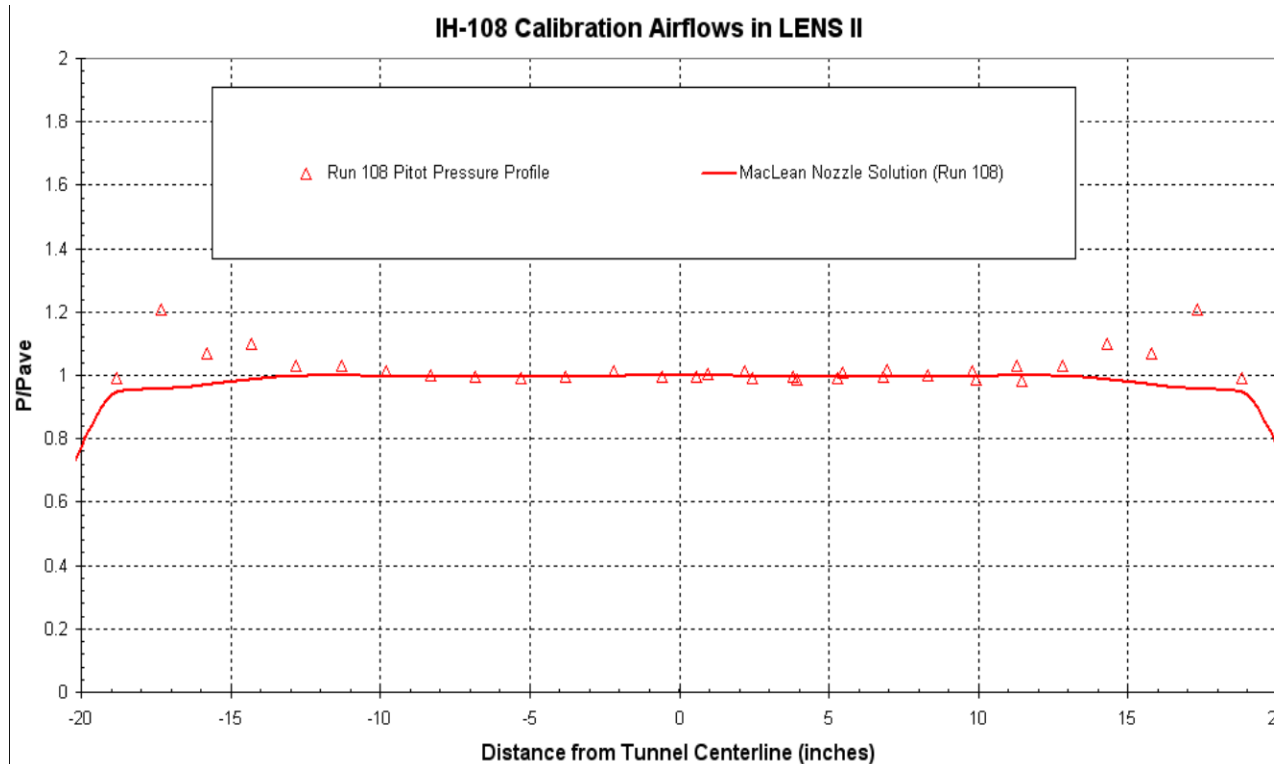
Hypersonic Design and Application



- Pitot Probes with High Frequency Gauges
- Calibration Ogive Model
  - 10% of the External Tank length including the aero-spike
  - Four (4) surface pressure gages on the 0° ray
  - Eight (8) heat transfer gages on the 180° ray



# Comparison of CFD vs. Measured Pitot Profile



- Flow Field Core About 36-Inches in Diameter at Exit Plane
- Pressure Profile Uniformity Within 2%

# Flow-field Evaluation Using ET Ogive Model

- **Boeing Pre-test Runs Using NPARC Alliance WIND Code**
  - Fully upwind van Leer flux splitting scheme for high Mach number flows
  - 2<sup>nd</sup> order spatial accuracy
  - Menter SST turbulence model
  - target cell Reynolds number ( $Y^+$ ) of 0.1
- **NASA JSC Post Calibration Runs Using OVERFLOW Code**
  - Menter SST turbulence model
  - Axi-symmetric Runs
- **CUBRC Post Calibration Runs Using DPLR Code**
  - Menter SST turbulence model
  - Assumed fully turbulent flow right from aero spike tip
  - Perfect gas simulation

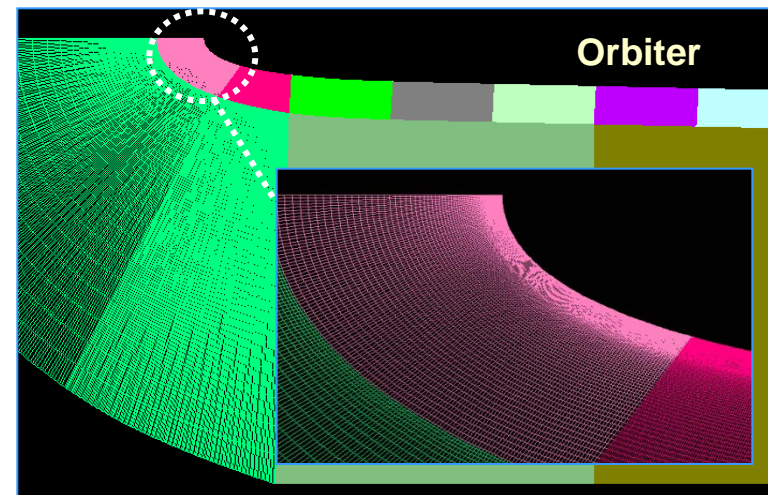
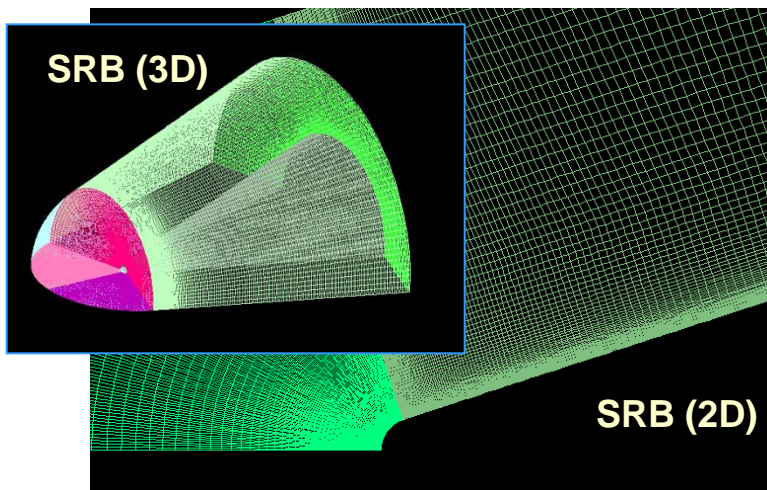
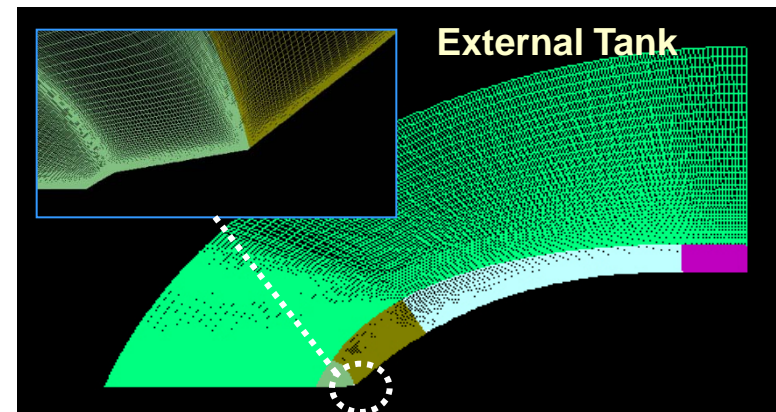
# Boeing WIND Code Solution Approaches

Advanced Global Strike Systems

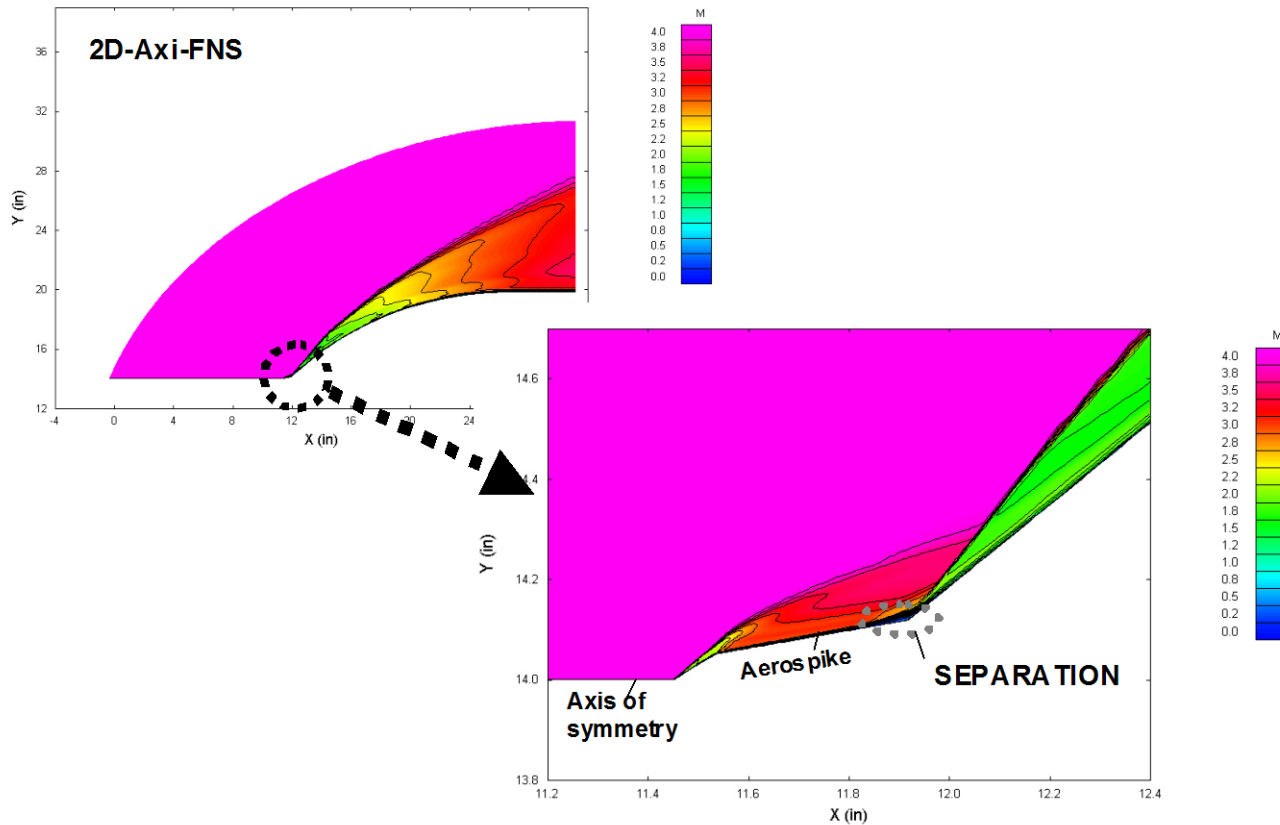
Hypersonic Design and Application

- Boeing WIND Code
- 2D Axisymmetric
- 3D
- FNS
- Structured Grid
- Liu-Vinokur Model
- SST Turbulence Model
- Inputs

IH-108 Test Mach Number  
IH-108 Test  $P_{inf}$  and  $T_{inf}$   
IH-108 Test  $T_{wall}$



# Typical ET Ogive Mach Number Contour in Mach 4.0 Turbulent Flow

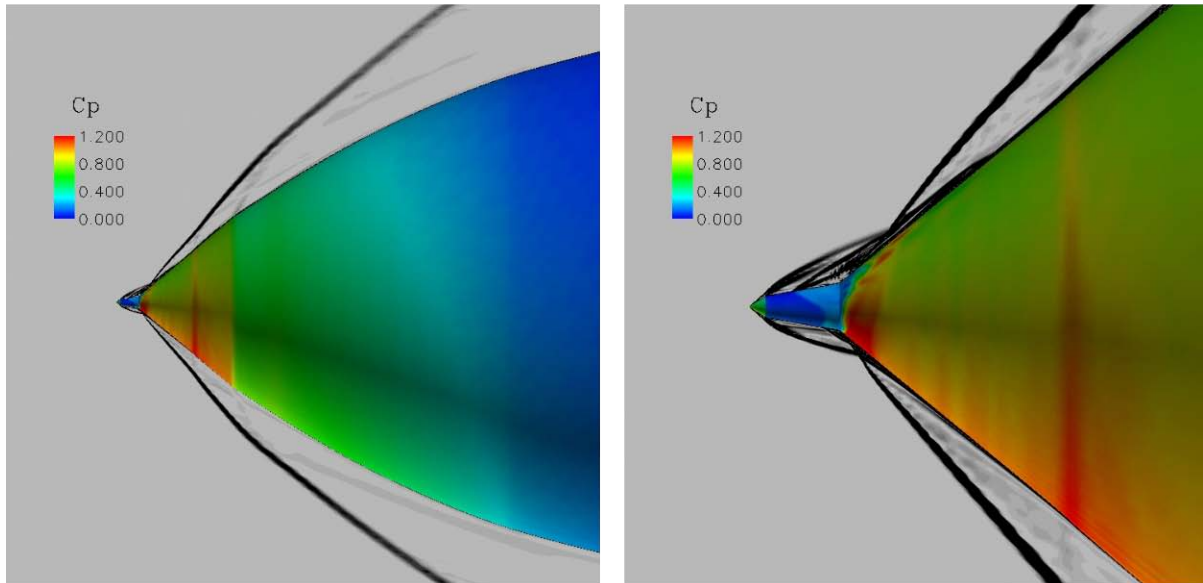


- WIND Optimized Grid Captured Shock Structure and Compression Corner Separation with Good Fidelity

# Laminar WIND Solution at Aero Spike Corner

Model Scale CFD (Laminar) To/Tw Conds.,  $M=4$ ,  $AoA=0$ ,  $\beta=0$

Pseudo-schlierens,  $C_p$  on body

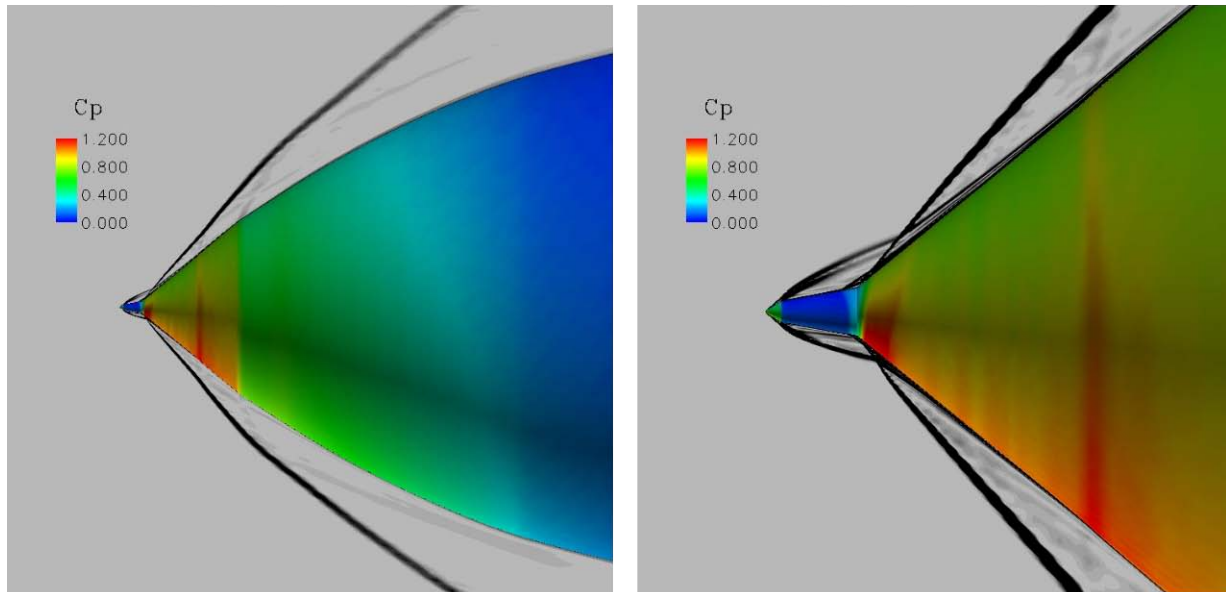


- **Massive Separation at Compression Corner Caused Unsteady Flow**

# Turbulent WIND Solution at Aero Spike Corner

Model Scale CFD (SST) To/Tw Conds.,  $M=4$ ,  $AoA=0$ ,  $\beta=0$

Pseudo-schlierens,  $c_p$  on body

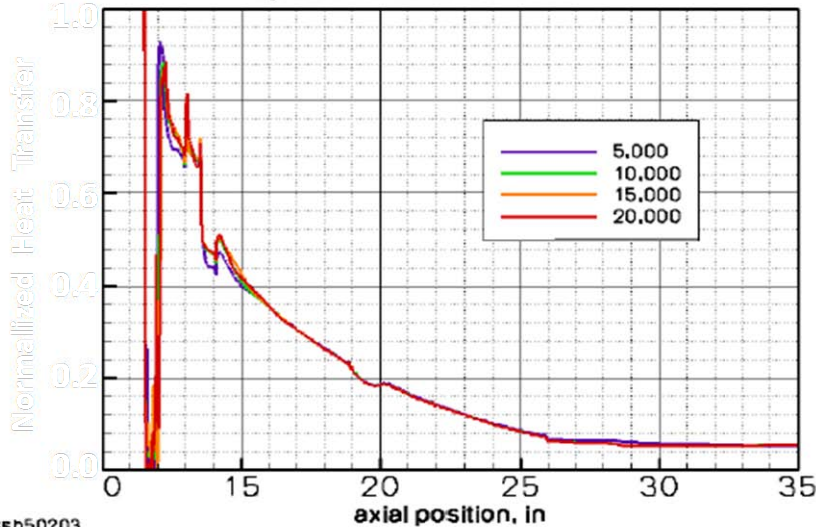


- **Turbulent CFD Schlieren Duplicated Wind Tunnel Test Schlieren Picture**

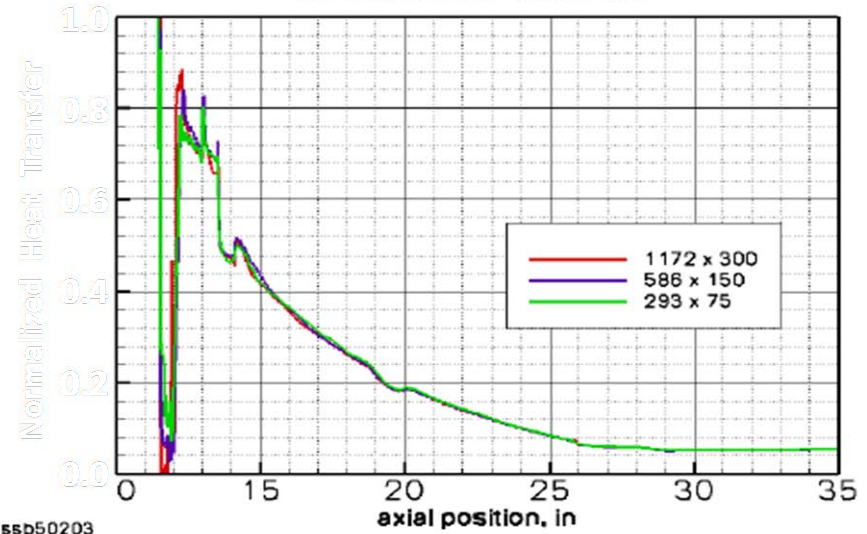


# DPLR Stable and Fast Converging

Convergence of Turbulent Heat Transfer Solution by iteration w/ DPLR Code



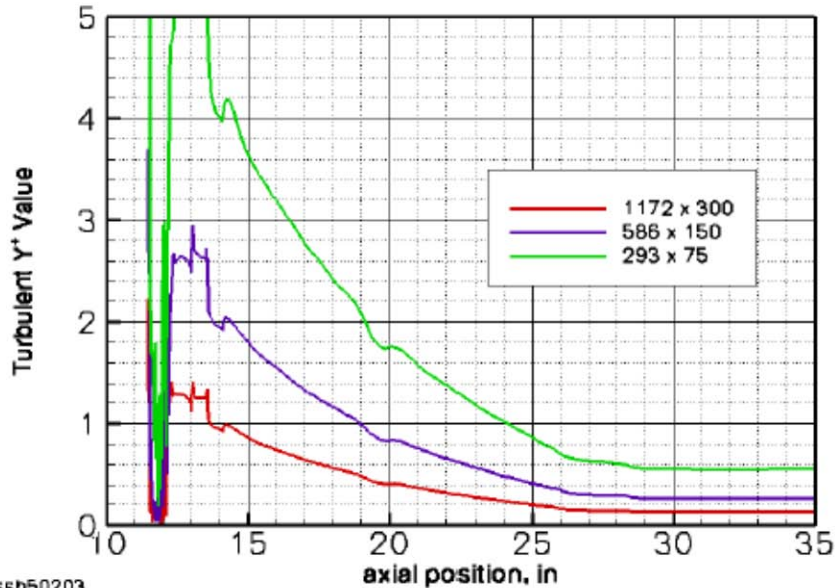
Ordered Discretization Error of Heat Transfer Solution on Axisymmetric OGIVE Grid



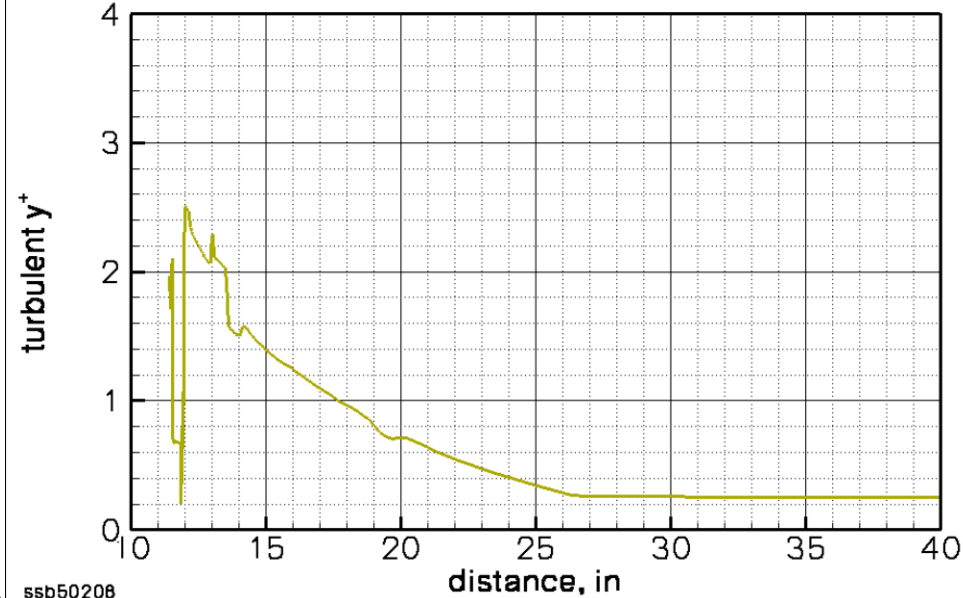
- **Grid Convergence and Discretization Error Addressed by Sequencing the Grid at Three Levels**
- **Some Grid Dependency in the Tri-cone Region Where the Flow Separates and Reattaches**
- **Solution Consistent Across All Three Grids on the Ogive Region**

# DPLR Shows Low Dependence on Grid Size

Near Wall Spacing by Grid Sequence



Turbulent Near-wall Cell Spacing



- DPLR Code Relatively Insensitive to Grid Sizing  $y^+$  Values
- Smallest Grid (293x75) Showed Sufficient Accuracy on Ogive Region
- Turbulent  $y^+$  Value Around 1 used for this Study

# Data Comparison Using Dimensionless Pressure and Heat Transfer

- Calibration Model is a Perfect Axi-Symmetric Ogive of Shuttle ET Nose Cone with the Aero Spike
- Pressure Coefficient

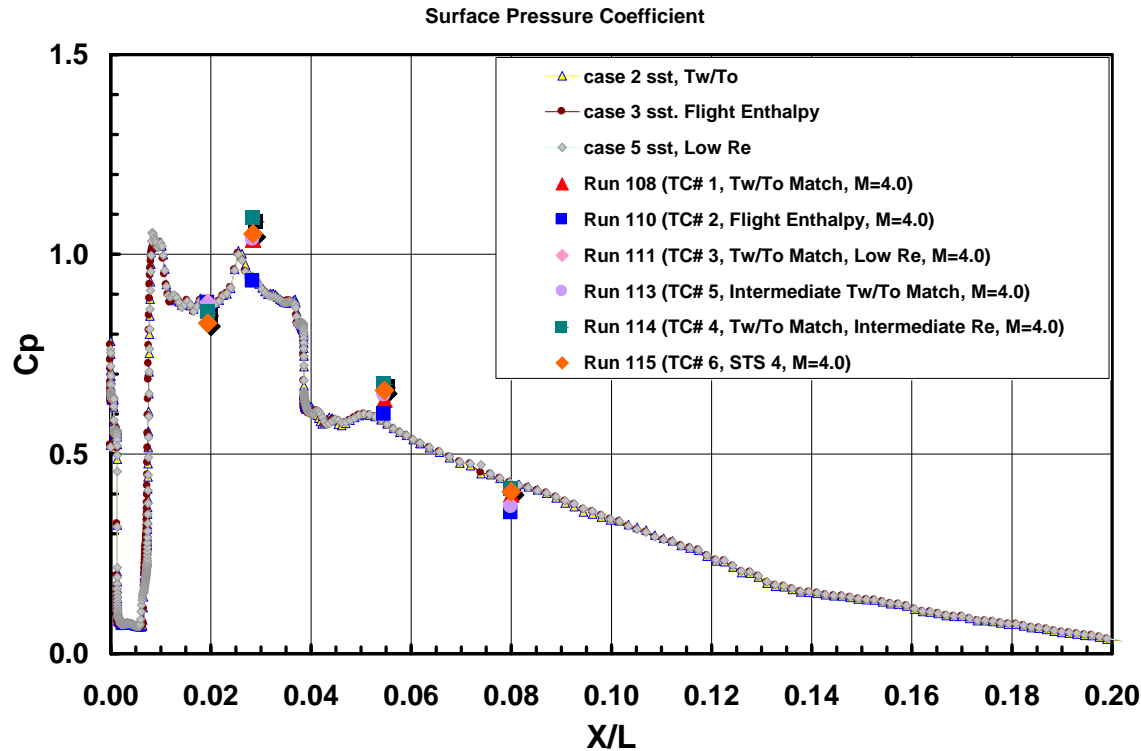
$$C_p = \frac{p - p_\infty}{\frac{\gamma}{2} M^2 p_\infty}$$

- Stanton Number

$$St = \frac{\dot{q}}{\rho_\infty V_\infty c_p (T_{aw} - T_w)}$$

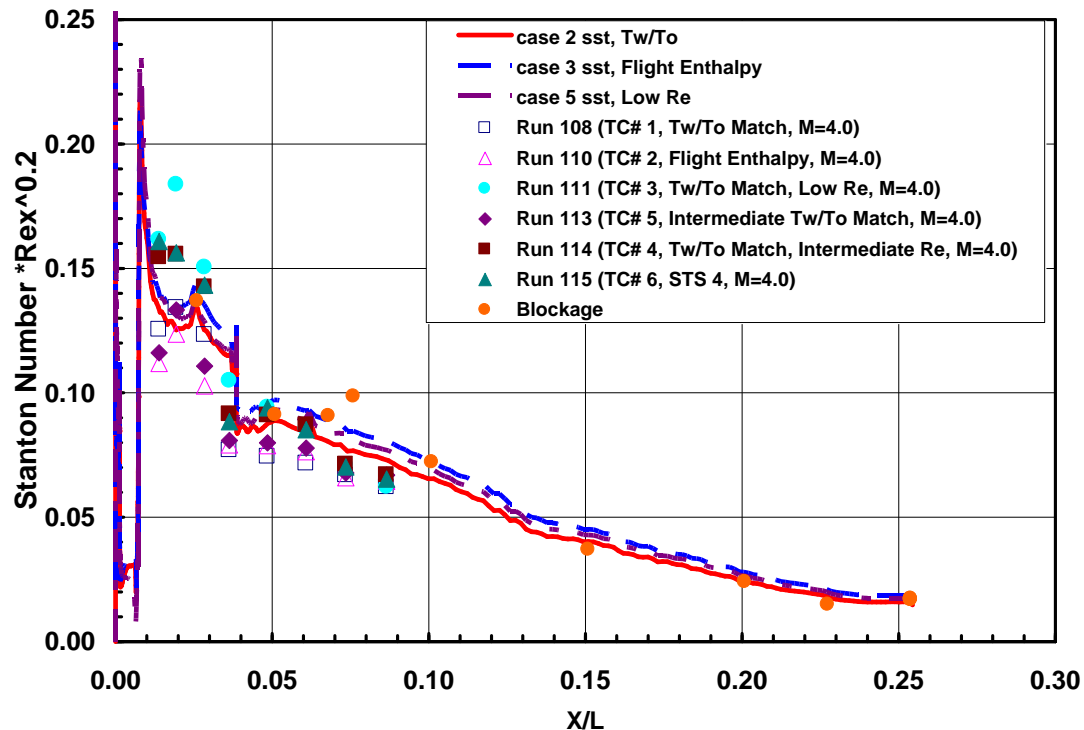
- Stanton Number x  $Re_x^{1/5}$

# WIND Code Pre-Test CFD Pressure Comparison with Calibration Runs



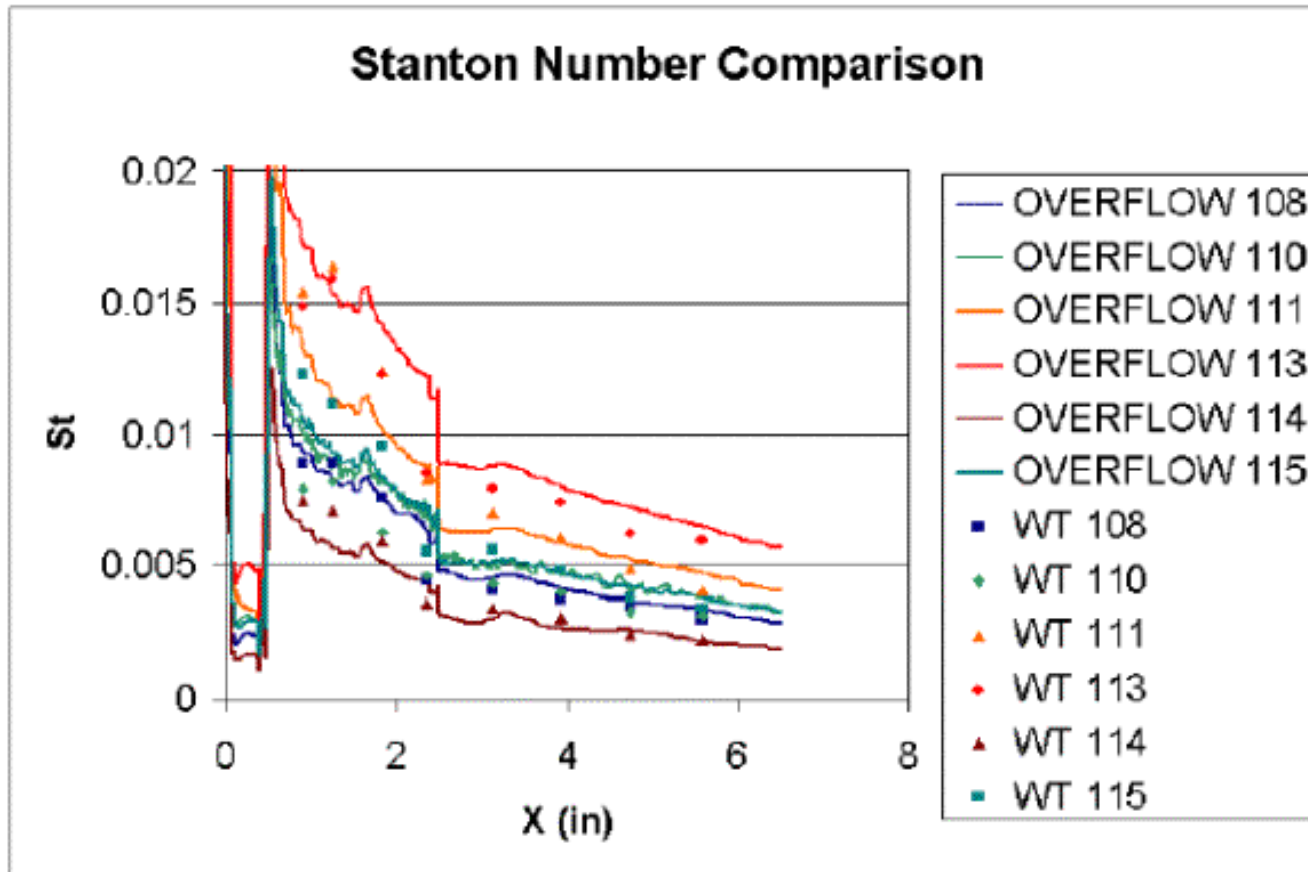
- Magnitude and Trend of Pressure Data Looked Good
- More Data Scatter Than Expected ( $\Delta C_p$ 's of 0.07 to 0.16 from run to run)
- Likely Result of Complex Flow at Aero Spike Corners

# WIND Code Pre-Test CFD Heat Transfer Comparison with Calibration Runs



- Stanton Number Times the  $1/5^{\text{th}}$  Power of the Local Reynolds Number,  $Re_x$ , Did Good Job of Collapsing Turbulent Data
- Run and Test Conditions Covered Wide Range of Reynolds Number and Total Pressure
- CFD Pretest Results Generally Over-predicted Slightly (~ 10%)

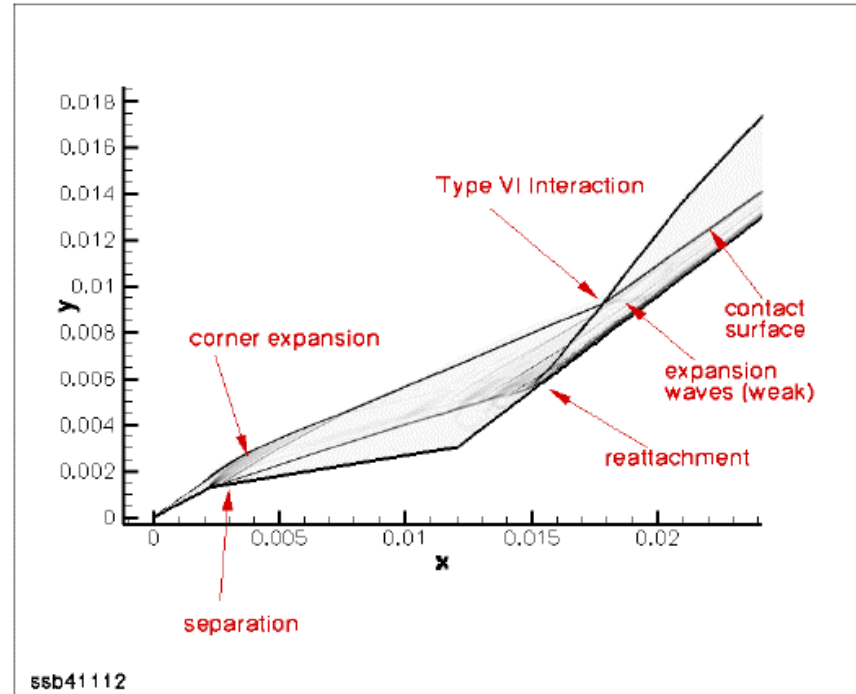
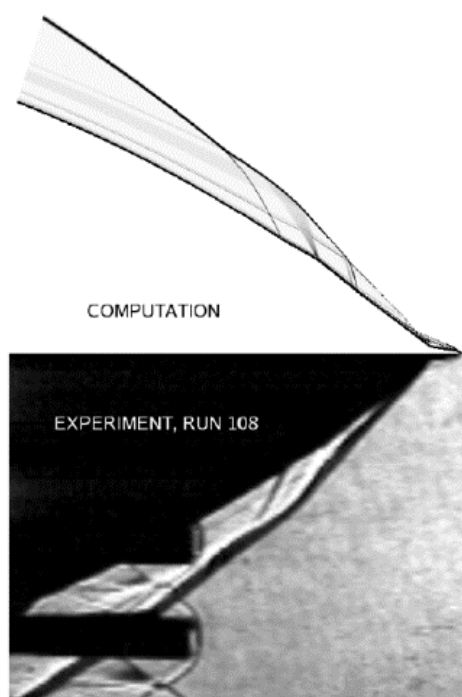
# OVERFLOW Code Post-Test CFD Heat Transfer Comparison with Calibration Runs



- CFD Solutions Used As-Run Conditions
- CFD Results Generally Over-predicted Slightly (~ 10%)



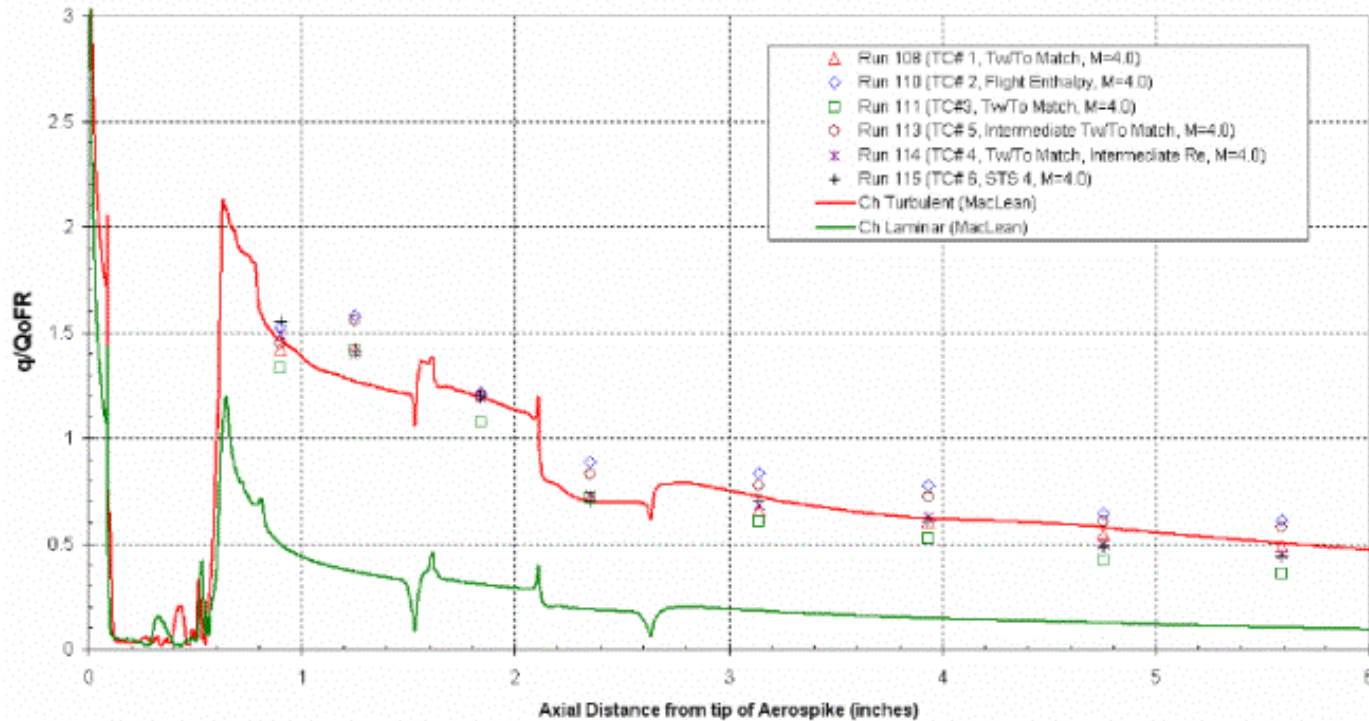
# DPLR Schlieren Shows Tri-Cone Flow Details



- Computational Schlieren and the Experimental Schlieren Shows Agreement within the Resolution of the Camera
- Computational Schlieren Shows Shock Interaction Patterns in Tri-Cone Region Which Defines Reattached Flow Field Downstream

# DPLR Code Post-Test CFD Heat Transfer Comparison with Calibration Runs

Calibration OGIVE Heat Transfer and Pressure Data

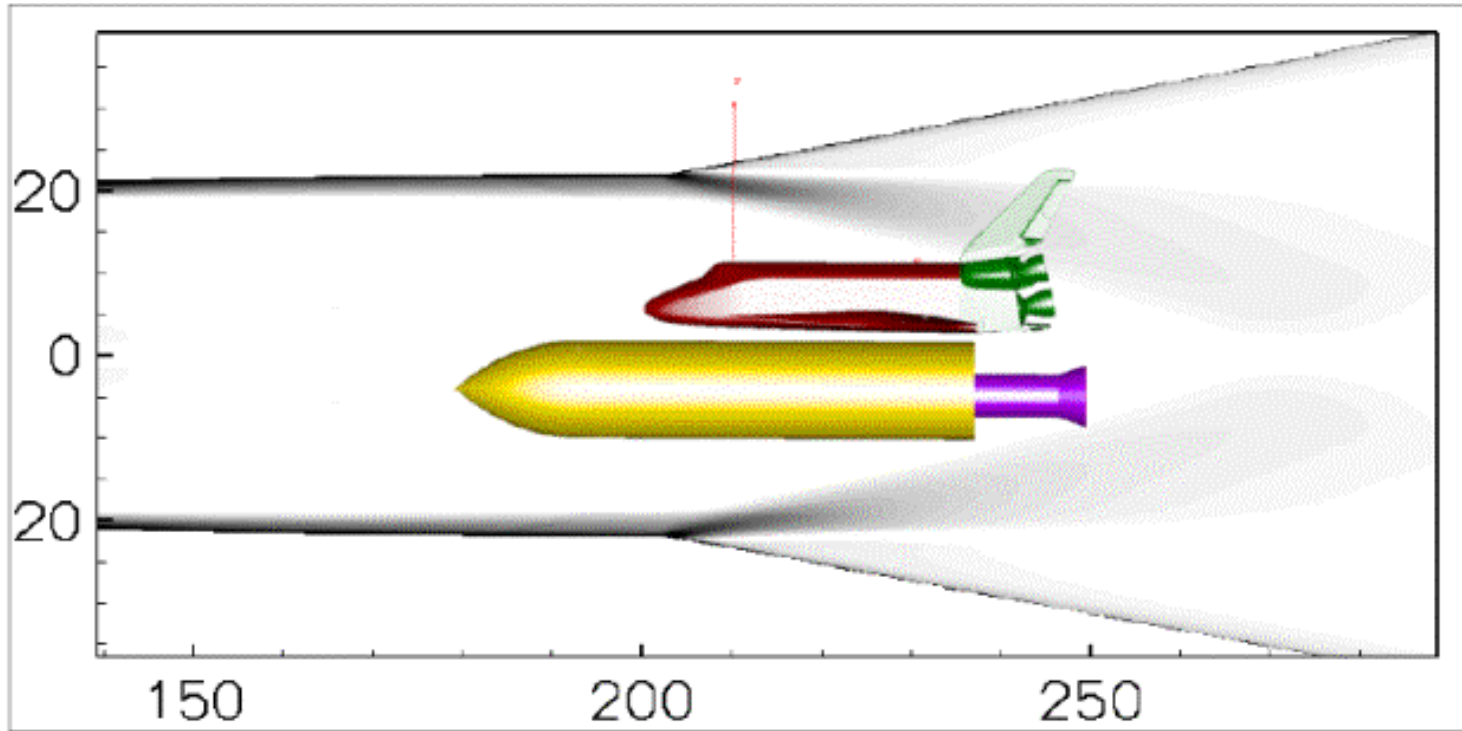


- CFD Solutions Used As-Run Conditions at Mach 4
- CFD Confirms the Flow Transitions to Turbulent Immediately Downstream of the Separation Reattachment

# Mach 4.0 Nozzle CFD Schlieren Plot with Super-Imposed Test Model (DPLR)

Advanced Global Strike Systems

Hypersonic Design and Application

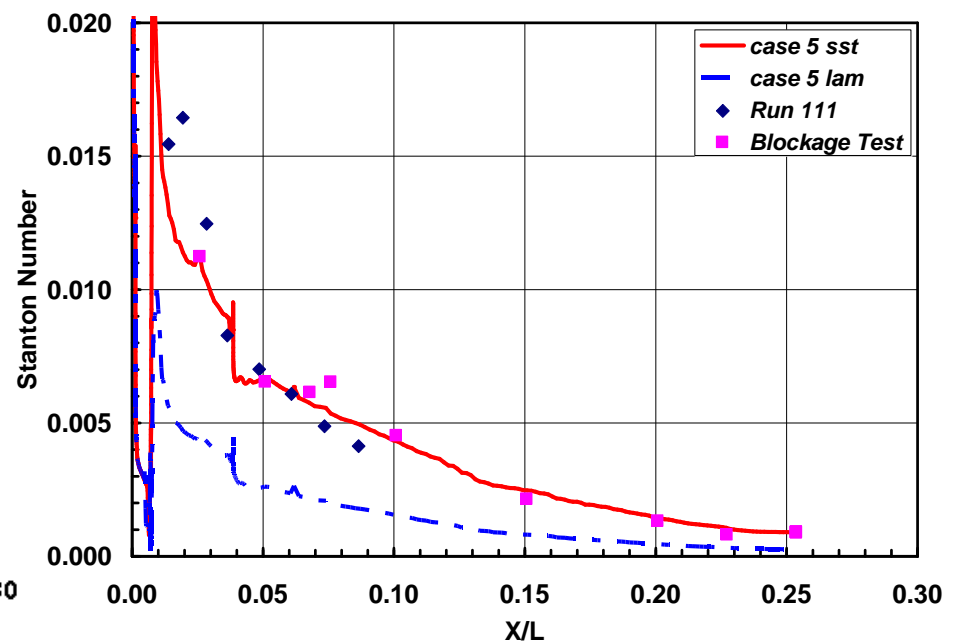
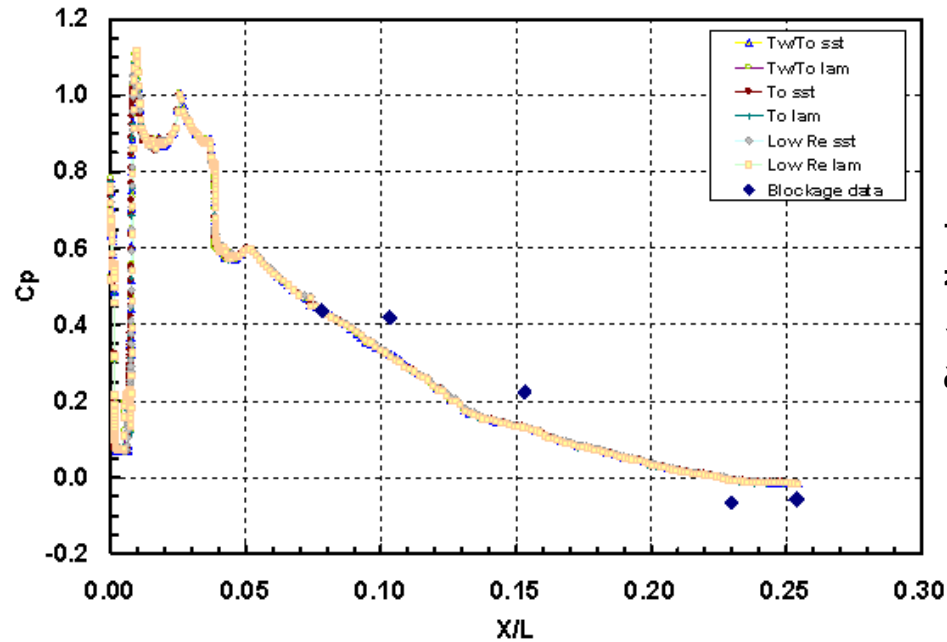


- **CFD Study Conducted to Alleviate Blockage Concern of Large Scale Integrated-Vehicle Model**
- **Expansion Waves Aft of Nozzle Wall Does Not Disrupt Forward and Bipod Region of Model**

# WIND Code Pre-Test CFD Solution Pressure Comparison with Blockage Run

Advanced Global Strike Systems

Hypersonic Design and Application



- **CFD Pressure Solutions Essentially Independent of Test Flow Conditions**
- **Calibration Model and Blockage Model Gauges Overlap**
- **Excellent Heat Transfer Comparison at Low Reynolds Number Conditions (Run 111 and blockage test, TC #3) Showing Turbulent Flow**

# IH-108 Test Boundary Layer State Analysis

- **Boundary Layer Characteristics In The Wind-tunnel Simulations Must Accurately Represent Those Seen In Flight**
- **WIND Code Pre-test CFD Cases Included Both Laminar And Turbulent Runs At Similar Free-stream Conditions**
- **Heat Transfer Measurements On The ET Ogive Model Confirmed That The Flow Was Fully Turbulent Immediately Downstream From Tri-Cone Interaction Region**
- **Separation At The Tri-cone Compression Corner Was Limited**
- **Turbulent Boundary Layer Existed On The ET Surface For All Test Conditions**

# Conclusions 1 of 2

- The requested free-stream test conditions were achieved within a reasonable range. The Mach 4.0 throat produces a very uniform test section Mach core with variation of 1% for 5 of the test conditions and one condition at 2% (Run 110, TC #2).
- For the Mach 4.0 test conditions, the agreement between calibration test data and CFD is very good. The test team felt confident that the desired test conditions had been simulated and sufficient calibration data were available to corroborate it.
- The calibration run heat transfer measurements on the ET ogive confirmed that the flow was fully turbulent immediately downstream from the location where the nose tip bow shock impinged on the ogive surface. Turbulent boundary layer also exists on the Orbiter windward surface in all test conditions. No boundary layer trip should be required for the ET or Orbiter model. The boundary layer state on the SRB, on the other hand, was not clearly defined by the test data.



# Conclusions 2 of 2

- **The availability of ET ogive pressure and heat transfer data before the actual test commenced provided a tremendous opportunity for pre-test run condition evaluation.**
- **All new test conditions using either new or existing nozzle hardware should be calibrated before the actual test is performed.**
- **Good agreement among the CFD solutions from Boeing, NASA/JSC and CUBRC team was shown. The predictions are consistent at all Mach 4 conditions and typically over-predicted the test data by 10% to 20% on the ET ogive.**